Struct Bond (2008) 126: 17–64
DOI 10.1007/430_2007_063

Published online: 19 September 2007

The Interaction of Dihalogens and Hydrogen Halides with Lewis Bases in the Gas Phase: An Experimental Comparison of the Halogen Bond and the Hydrogen Bond

A. C. Legon

School of Chemistry, University of Bristol, Bristol BS8 1TS, UK
A.C.Legon@Bristol.ac.uk

Abstract This chapter is concerned exclusively with the experimentally determined properties of halogen-bonded complexes of the type B···XY in isolation in the gas phase and their relationship with those of the corresponding hydrogen-bonded complexes B···HX.

B is one of a series of simple Lewis bases and XY is a homo- or hetero-dihalogen molecule F_2, Cl_2, Br_2, ClF, BrCl or ICl. The method used to determine these properties (angular and radial geometry, binding strength, and the extent of electric charge redistribution on formation of B···XY) is first outlined. A comparison of the angular geometries of the pair of halogen-bonded and hydrogen-bonded complexes B···ClF and B···HCl as B is systematically varied follows. Systematic relationships among the radial geometries of the two series are also summarised. The intermolecular stretching force constants k_σ and the extent of electron transfer (both inter- and intramolecular) on formation of B···XY, for XY = Cl_2, Br_2, ClF, BrCl or ICl, are shown to vary systematically as B is varied. A striking similarity noted among the properties of halogen-bonded complexes B···XY and their hydrogen-bonded analogues B···HX demonstrates that rules for predicting the angular geometries of hydrogen-bonded complexes (and other generalisations) may also be applied to the halogen-bonded series, but with the caveat that while the hydrogen bond shows a propensity to be non-linear when B···HX has appropriate symmetry, the halogen bond tends to remain close to linearity. A model for the halogen bond, successfully applied earlier to the hydrogen bond, is proposed.

Keywords Lewis bases · Dihalogens · Halogen bond · Angular geometry · Electric charge transfer

Abbreviations

Efg	Electric field gradient
n-pair	Non-bonding electron pair
π-pair	π-bonding electron pair
XY	Generalised dihalogen molecules
HX	Generalised hydrogen halide

1 Introduction

This chapter is restricted to a discussion of halogen-bonded complexes B···XY that involve a homo- or hetero-dihalogen molecule XY as the electron acceptor and one of a series of simple Lewis bases B, which are chosen for their simplicity and to provide a range of electron-donating abilities. Moreover, we shall restrict attention to the gas phase so that the experimental properties determined refer to the isolated complex. Comparisons with the results of electronic structure calculations are then appropriate. All of the experimental properties of isolated complexes B···XY considered here result from interpreting spectroscopic constants obtained by analysis of rotational spectra.

1.1 Historical Background

The first report of an adduct of the type to be discussed here was that of Guthrie in 1863 [1], who described the compound $H_3N\cdots I_2$. The spectroscopy of the interaction of benzene with molecular iodine in the UV/visible

region carried out by Benesi and Hildebrand in 1949 [2] was the initial focus of the important work of Mulliken [3] on the theory of electron donor–acceptor complexes in the 1950s and 1960s. During that period, Hassel and co-workers [4, 5] carried out X-ray diffraction studies of crystals of addition complexes formed by dihalogen molecules with Lewis bases. They concluded that the hydrogen bridge and halogen bridge were closely related. Of particular interest in the context of the work to be described here is Hassel's statement that, in complexes formed between halogen molecules and electron-donor molecules possessing lone pairs of electrons, it is to be assumed "that halogen atoms are directly linked to donor atoms with bond directions roughly coinciding with the axes of the orbitals of the lone pairs in the non-complexed donor molecule". Hassel's investigations involved crystals of the adducts, so that the complexes were therefore mutually interacting, albeit quite weakly. Complexes in effective isolation in cryogenic matrices were studied by infrared spectroscopy in the 1980s, particulary by Pimentel [6], Ault [7–10] and Andrews [11–14]. The so-called fast-mixing nozzle [15] incorporated into a pulsed-jet, Fourier-transform microwave spectrometer [16, 17] allowed complexes formed from simple Lewis bases (such as NH_3, H_2CCH_2, etc.) and dihalogen molecules to be isolated and probed by microwave radiation before they could undergo the (sometimes violent) reaction that attends normal mixing. This technique allowed the power and precision of rotational spectroscopy to be brought to bear on many simple complexes. Moreover, the Lewis base and the dihalogen molecule could be systematically varied to reveal conclusions of general interest about the binding that holds the two components together.

1.2 Definitions and Nomenclature

The aim of this chapter is to show that there is a strong parallelism between the measured properties of halogen-bonded and hydrogen-bonded complexes and, consequently, that the terms *halogen bond* and *hydrogen bond* carry similar connotations. After extensive consultations and discussions, the IUPAC Working Party on the hydrogen bond, and other molecular interactions, put forward the following definition of the hydrogen bond for consideration by the Chemistry community [18]:

"*The hydrogen bond is an attractive interaction between a group X–H and an atom or a group of atoms, in the same or different molecule(s), when there is evidence of bond formation.*"

Of several properties simultaneously recommended as providing criteria of such evidence, the most important in the present context are:

1. The physical forces involved in the hydrogen bond must include electrostatic and inductive forces in addition to London dispersion forces

2. The atoms H and X are covalently bound to one another, and B···HX is polarised so that the H atom becomes more electropositive (i.e. the partial positive charge $^{\delta+}$ increases)
3. The lengths of the H–X bond and, to a lesser extent, the bonds involved in B deviate from their equilibrium values
4. The stronger the hydrogen bond, the more nearly linear is the Z···H – X arrangement and the shorter the B···H distance
5. The interaction energy per hydrogen bond is greater than at least a few times kT, where T is the temperature of the observation, in order to ensure its stability

We shall show both from experimental evidence about gas-phase complexes and, to a lesser extent, from the results of electronic structure calculations that a parallel definition of the intermolecular halogen bond is appropriate:

"*The halogen bond is an attractive interaction between a halogen atom X and an atom or a group of atoms in different molecule(s), when there is evidence of bond formation.*"

The atom X may be attached to another halogen atom Y or some other group of atoms R and the criteria (1–5) can be used with appropriate modification.

This definition was implied by the author [19, 20], who used the terms halogen bond or chlorine bond in these and in earlier articles referred to therein. The definition is also similar to that proposed by Metrangolo et al. [21], who used the term halogen bond (with XB as an abbreviation analogous to HB for the hydrogen bond) to describe any non-covalent interaction involving halogens as electron acceptors. Thus, the general notation for the halogen bond would be B···XY, where B is a Lewis base (electron donor), X is a halogen atom (electron acceptor) and Y can be a halogen atom or some other atom that is a constituent of a group R attached to X. The Lewis base B and XY might undergo a chemical reaction when mixed under normal conditions of temperature and pressure. This is especially so when XY is F_2 or ClF, both of which are notoriously reactive. To obtain the experimental results discussed here, pre-mixing of the components was avoided and instead we used a coaxial flow technique [15] to form B···XY but to preclude chemical reaction of B and XY. Accordingly, the phrase *pre-reactive complexes* is used to describe such species [22].

Mulliken [3] presented a classification of electron donor–acceptor complexes based on the extent of intermolecular charge transfer that accompanies complex formation. An *outer* complex is one in which the intermolecular interaction B···XY is weak and there is little intra- or intermolecular electric charge redistribution, while an *inner* complex is one in which there is extensive electric charge (electrons or nuclei) redistribution to give $[BX]^+\cdots Y^-$. Inner complexes are presumably more strongly bound in general than outer complexes.

1.3 Summary

The structure of the remainder of this chapter is as follows: First, in Sect. 2, we shall summarise briefly how the various properties of isolated complexes B···XY may be derived from the molecular constants that are determinable by analysis of rotational spectra. Then, in Sects. 3, 4 and 5, we shall present some generalisations about the halogen bond through the discussion of pre-reactive, outer complexes of the type B···XY. The approach will be to compare the properties of halogen-bonded complexes B···XY, as determined from rotational spectroscopy, with those of the corresponding hydrogen-bonded analogues B···HX, similarly determined. We shall show by systematic variation of both B and XY that there is a striking parallelism of the properties (angular geometry in Sect. 3, intermolecular stretching force constant in Sect. 4, electric charge redistribution on complex formation in Sect. 5) between the two types of complex. We shall also show in Sect. 5, by a comparison of the series $H_3N\cdots HX$ and $(CH_3)_3N\cdots HX$ with corresponding members of the series $H_3N\cdots XY$ and $(CH_3)_3N\cdots XY$, that hydrogen- and halogen-bonded complexes that tend towards the limiting Mulliken inner type can be identified in the gas phase and that there is here also a strong analogy between the two classes of complex. In conclusion, in Sect. 6, we shall indicate that a simple, essentially electrostatic model for the hydrogen bond is also appropriate for the halogen bond in outer complexes.

2 Properties of Isolated Complexes B···XY: How to Measure Them

Rotational spectroscopy is a precise means by which the properties of molecules in effective isolation in the gas phase may be measured. Only for strong complexes (particularly those linked by a hydrogen bond) have rotational spectra been detected by using equilibrium gas mixtures of the two components at normal or slightly lower temperatures [23]. Techniques that involve supersonic jets or beams are usually employed when the rotational spectra of more weakly bound species are sought. The two methods most used in this context are molecular beam electric resonance spectroscopy (MBERS) and pulsed-jet, Fourier-transform (F-T) microwave spectroscopy, both of which have been described in detail elsewhere [16, 17, 24]. A supersonic jet or beam of gas mixture is formed by expanding a mixture of the components of interest (e.g. B and XY here) in, e.g., excess argon through a small circular hole (nozzle) into a vacuum. When the gas pulse enters the vacuum chamber it is rich in weakly bound complexes, which achieve collisionless expansion after ca. 10 μs. Thereafter, the target species are frozen in their lowest rotational states and usually in the zero-point vibrational state

until they undergo collision with the walls of the vacuum chamber. The complexes can absorb microwave radiation while in the collisionless expansion phase and their rotational spectra can be detected. The results presented here have been established mainly by using a pulsed-nozzle, F-T microwave spectrometer, but modified to incorporate a so-called fast-mixing nozzle [15]. The latter device allows complexes of B···XY to be formed from two reactive components B and XY (e.g. ethyne and ClF) and achieve collisionless expansion in the vacuum chamber before the reaction (often violent) that would attend mixing under normal conditions. A detailed description of this nozzle is available elsewhere [25].

The form of the observed spectrum of B···XY can often give a clue to the symmetry of the species responsible for it. Thus asymmetric-top molecules, symmetric-top molecules and linear molecules give rise to different spectral patterns. Once the rotational spectrum of a complex B···XY has been assigned, the observed transition frequencies may be fitted to give a range of precise spectroscopic constants, usually for the zero-point state, which can then be interpreted to give various molecular properties of B···XY. Of principal interest here are the rotational constants, centrifugal distortion constants and nuclear quadrupole coupling constants.

Rotational constants $G = A$, B or C are inversely proportional to principal moments of inertia I_α through the expressions $G = h/8\pi^2 I_\alpha$, where α refers to one of the three principal inertia axis directions a, b or c. The I_α are related to the coordinates of the atoms i in the principal axis system via the relations $I_\alpha = \sum_i m_i(\beta_i^2 + \gamma_i^2)$, where α, β and γ are to be cyclically permuted over a, b and c. Hence, the principal moments of inertia are simple functions of the distribution of the masses of the atoms of the complex in space. Accordingly, these quantities can be used to determine the separation of the two subunits B and XY and their relative orientation in space, i.e. the radial and angular geometries of the complex, respectively. All molecular geometries of B···XY considered here are of the r_0-type, that is, are obtained by fitting the zero-point principal moments of inertia of a limited number of isotopomers as though they are equilibrium quantities. Moreover, the geometry of each component is assumed to survive complex formation.

Although there are several centrifugal distortion constants that can be determined from the rotational spectrum of a complex B···XY, one is of special importance, namely, D_J (for linear or symmetric top molecules) or, equivalently, Δ_J (for an asymmetric-rotor molecule). Both D_J and Δ_J are inversely proportional to the intermolecular stretching force constant k_σ, according to simple and convenient expressions presented by Millen [26] in the approximation of rigid, unperturbed subunits B and X and with the neglect of terms higher than quadratic in the intermolecular potential energy function. Thus, k_σ offers a measure of the strength of the interaction, given that it is the restoring force per unit infinitesimal extension of the weak bond.

The final spectroscopic constants of particular interest here are the halogen nuclear quadrupole coupling constants $\chi_{\alpha\beta}(X)$ and $\chi_{\alpha\beta}(Y)$ [27], where α and β are to be permuted over the principal inertial axis directions *a*, *b* and *c*. Halogen nuclei (with the exception of ^{19}F) have an intrinsic (or spin) angular momentum, $\boldsymbol{I}_X$, with a spin quantum number $I_X \geq 3/2$ and therefore with a non-zero electric quadrupole moment $\mathbf{Q}_X$. The nuclear spin vector $\boldsymbol{I}_X$ can couple in only a limited number of discrete orientations to the rotational angular momentum vector $\boldsymbol{J}$ of the molecular framework. Each allowed orientation of the angular momentum and spin vector corresponds to different orientations of the nuclear electric quadrupole moment with respect to the electric field gradient $\nabla\mathbf{E}_X$ at X and therefore to a different interaction energy. Hence, rotational energy levels (and therefore transitions) carry a hyperfine structure. Analysis of this nuclear quadrupole hyperfine structure gives various components (depending on the molecular symmetry) of the nuclear quadrupole coupling tensor $\chi_{\alpha\beta}(X)$, where α and β are to be permuted over the principal inertial axes *a*, *b* and *c*. The importance of this tensor follows from its definition $\chi_{\alpha\beta}(X) = -(eQ_Xh)\partial^2 V_X/\partial\alpha\partial\beta$ where Q_X is the conventional electric quadrupole moment of nucleus X and $-\partial^2 V/\partial\alpha\partial\beta$ is a component of the electric field gradient (efg) tensor at the nucleus X. This direct proportionality of $\chi_{\alpha\beta}(X)$ and $\chi_{\alpha\beta}(Y)$ to the efgs at the nuclei X and Y, respectively, means that the changes $\Delta\chi_{\alpha\beta}(X)$ and $\Delta\chi_{\alpha\beta}(Y)$ in $\chi_{\alpha\beta}(X)$ and $\chi_{\alpha\beta}(Y)$ that accompany formation of B···XY lead directly to the changes in the efgs at X and Y. Hence $\Delta\chi_{\alpha\beta}(X)$ and $\Delta\chi_{\alpha\beta}(Y)$ carry quantitative information about the electric charge redistribution associated with the process. We shall see in Sect. 5 that intra- and intermolecular electron transfer on formation of B···XY can be estimated from these quantities. For an asymmetric rotor of C_S symmetry, only one off-diagonal element (*ab* or *ac* normally) of the tensor $\chi_{\alpha\beta}(X)$ or $\chi_{\alpha\beta}(Y)$ is non-zero but its value provides important information about the orientation of the XY subunit with respect to the principal inertial axis system (*a*, *b*, *c*) in complexes B···XY (and indeed of the HX subunit in hydrogen-bonded complexes B···HX [28, 29]). This leads to an estimate of the deviation of the Z···X – Y (or Z···H — X) atoms from collinearity, where Z is the electron-donor atom of B, as discussed in Sect. 3.

3
Comparison of the Angular and Radial Geometries of Halogen-Bonded Complexes B···XY and their Hydrogen-Bonded Analogues B···HX

In this section, we discuss the observed geometries, both angular (the relative orientation of the components B and XY in space) and radial (the distance between B and XY at the observed orientation) of complexes B···XY.

Attention will be paid to the systematic relationship of the geometries of B···XY to those of hydrogen-bonded complexes in the corresponding series B···HX, especially for angular geometries, which are dealt with in detail in Sects. 3.1, 3.2 and 3.3. Radial geometries are treated only in summary (Sect. 3.4) here, but a detailed analysis is available in [19].

Many complexes B···XY, where B is a Lewis base and XY is F_2, [30–37], Cl_2 [22, 38–48], BrCl [49–58], ClF [34, 59–85], Br_2 [86–92] or ICl [93–102], have been investigated by means of their rotational spectra. Those in the group B···ClF cover the largest range of Lewis bases B, mainly because ClF contains only a single quadrupolar nucleus and the rotational spectra are relatively simple. Except for F_2, all the other dihalogen molecules contain two quadrupolar nuclei and hence the rotational transitions of the B···XY complexes display complicated nuclear quadrupole hyperfine structure. For this reason, the complexes B···Cl_2, B···BrCl, B···Br_2 and B···ICl investigated have been limited mainly to those of relatively high symmetry (molecular point groups $C_{\infty v}$, C_{2v} and C_{3v}), which simplifies the spectral analysis. Necessarily, these complexes yield more information about the electric charge redistribution that accompanies complex formation (Sect. 5).

It will be shown in Sect. 5.1 that the extent of electron transfer to XY from B and the extent of electron transfer within XY when B···XY is formed are both small in most complexes so far investigated in the gas phase. Members of this group also have small intermolecular stretching force constants k_σ and are weakly bound (see Sect. 4). Such complexes are therefore of the Mulliken outer type and the discussion of geometries here will be limited to these. There are a few complexes B···XY that exhibit significant electric charge rearrangement and are strongly bound. This group can be categorised as approaching the Mulliken inner complex limit and will be discussed in Sect. 5.2.

The discussions of Sects. 3.1, 3.2 and 3.3 are structured by reference to a set of rules that were proposed some years ago [103, 104] for rationalising the angular geometries of hydrogen-bonded complexes of the type B···HX, where X is a halogen atom. These rules are as follows:

The equilibrium angular geometry of a hydrogen-bonded complex B···HX can be predicted by assuming that the axis of the HX molecule lies:

1. Along the axis of a non-bonding (n) electron pair carried by the acceptor atom of B, with $^{\delta+}$H closer to the n-pair than $X^{\delta-}$, or
2. Along the local symmetry axis of a π- or pseudo-π orbital (with $^{\delta+}$H interacting with the π-density) when B carries no n-pairs, or
3. Along the axis of a n-pair, when B carries both n- and π-pairs (i.e. rule 1 takes precedence over rule 2 in this case)

Guided by these rules, we shall compare in most detail the observed angular geometries of pairs of complexes B···ClF and B···HCl for a wide range of Lewis bases B, although we shall also refer to other B···XY and B···HX. The reasons for choosing B···HCl and B···ClF as the series of halogen- and hydrogen-bonded complexes for comparison are: (i) that these are by far the most systematically studied of all the pairs of B···HX/B···XY series and (ii) that deviations of the hydrogen bond atoms Z···H – Cl from collinearity have been determined for a number of B···HCl of C_S symmetry and are available for comparison with the corresponding quantity for B···ClF, similarly determined. For each complex, the geometry was obtained by fitting the principal moments of inertia of one or more isotopomers under the assumption of unperturbed monomer geometries.

3.1
Angular Geometries of B···ClF and B···HCl in Which B is a n-Pair Donor

We begin by comparing pairs of B···ClF and B···HCl that test rule 1. We shall show a diagram comparing the experimental geometries, drawn to scale, of B···ClF and B···HCl for each B, together with a representation of B, also to scale but with its n-pair(s) drawn in the form of an exaggerated electron density distribution that is traditionally used among chemists. We shall then employ a similar approach for various prototype π-electron donors to test rule 2 and for mixed n- and π-donors appropriate to rule 3 in Sects. 3.2 and 3.3, respectively.

3.1.1
B Carries a Single n-Pair

The prototype Lewis base that carries a single n-pair and no π-pairs is ammonia. The observed geometries of $H_3N···ClF$ [63] and $H_3N···HCl$ [105] are shown in Fig. 1, as is the n-pair model of NH_3. Both complexes are symmetric-top molecules belonging to the C_{3v} molecular point group and clearly both obey rule 1. The geometries of the complexes $H_3N···F_2$ [30], $H_3N···Cl_2$ [45], $H_3N···BrCl$ [52], $H_3N···Br_2$ [86] and $H_3N···ICl$ [97] were found also to be of C_{3v} symmetry and isomorphous with their $H_3N···HX$ counterparts (X = F [1], Cl [105], Br [106] and I [107]). The halogen atom of higher atomic number acts as the electron acceptor in complexes containing a heteronuclear dihalogen molecule. The same conclusions have been reached for the pairs $H_3P···XY$, for XY = Cl_2 [40], BrCl [55], Br_2 [88] and ICl [102], and their H-bonded analogues $H_3P···HX$, where X = Cl [108], Br [109] and I [110].

[1] Howard BJ, Langridge-Smith PPR, unpublished observations

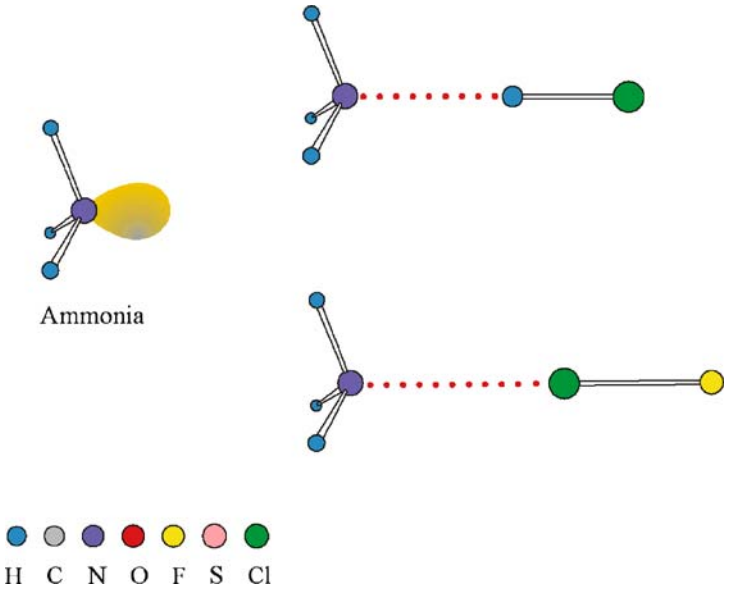

Fig. 1 Comparison of the experimentally determined geometries of the hydrogen-bonded complex $H_3N\cdots HCl$ and its halogen-bonded analogue $H_3N\cdots ClF$ (both drawn to scale) with a non-bonding electron-pair (n-pair) model of NH_3. Here, and in other figures, the n-pair electron distribution is drawn in the exaggerated style favoured by chemists. The key to the colour coding of atoms used in this and similar figures is also displayed

3.1.2
B Carries Two Equivalent n-Pairs

3.1.2.1
Linear Halogen Bonds and Hydrogen Bonds

The prototype Lewis bases in this category are H_2O and H_2S. The complex $H_2O\cdots HF$ is sufficiently strongly bound to have been investigated in an equilibrium mixture of H_2O and HF held at 200 K in the cell of a conventional Stark-modulation microwave spectrometer [111, 112]. This allowed vibrational satellites associated with low-frequency, intermolecular stretching and bending modes to be observed and analysed and vibrational wavenumbers for these modes to be determined. It was not only possible to conclude that in the zero-point state this complex is effectively planar but also to determine the potential energy (PE) as a function of the out-of-plane, low-frequency, hydrogen-bond bending co-ordinate. The mode in question inverts the configuration at the oxygen atom and is shown schematically in Fig. 2. The $O\cdots H-F$ nuclei were assumed to remain collinear during this motion. The energy levels associated with the motion were calculated by using the ex-

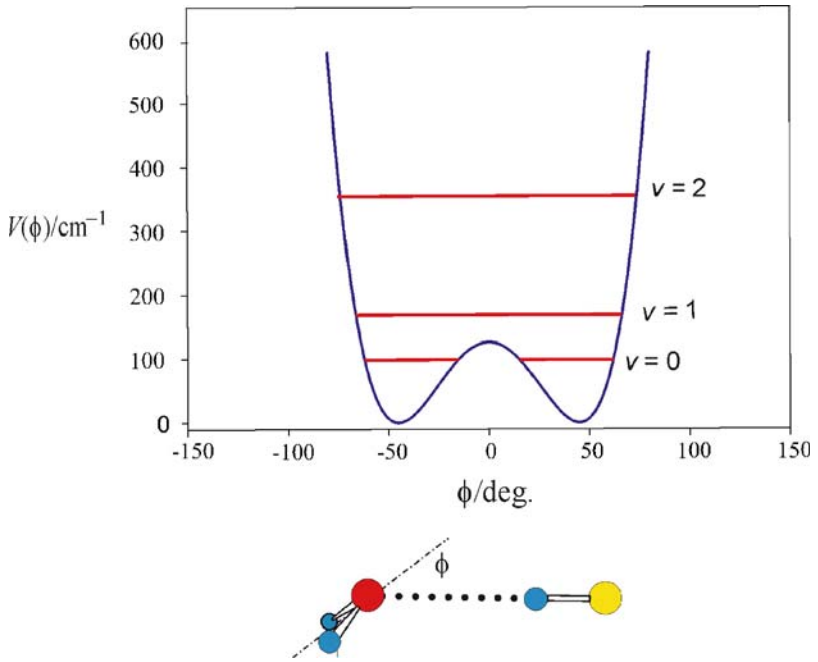

Fig. 2 The experimentally determined potential energy $V(\phi)$, expressed as a wavenumber for convenience, as a function of the angle ϕ in the hydrogen-bonded complex $H_2O\cdots HF$. The definition of ϕ is shown. The first few vibrational energy levels associated with this motion, which inverts the configuration at the oxygen atom, are drawn. The PE barrier at the planar conformation ($\phi = 0$) is low enough that the zero-point geometry is effectively planar (i.e. the vibrational wavefunctions have C_{2v} symmetry, even though the equilibrium configuration at O is pyramidal with $\phi_e = 46°$ (see text for discussion)). See Fig. 1 for key to the colour coding of atoms

pression for the conventional quartic/quadratic PE function in terms of the dimensionless reduced coordinate z given in Eq. 1. This function was fitted to a range of experimental data to give the potential constants a and b and then converted to the equivalent ϕ-dependent form of the type given in Eq. 2, where ϕ is the inversion angle defined in Fig. 2. The form of the reduced mass for the inversion motion and details of the calculation are given in [112]:

$$V(z) = a(z^4 - bz^2) \tag{1}$$

$$V(\phi) = A\phi^4 - B\phi^2 \tag{2}$$

We note from Fig. 2 that the hypothetical equilibrium conformation is pyramidal, with $\phi_e = 46(8)°$, even though the geometry of the complex is effectively planar in the zero-point state (i.e. the vibrational wavefunction has C_{2v} symmetry) because the PE barrier at the planar ($\phi = 0$) form is low. At the time of the publication of [112] this was a critical result because it demon-

strated that rule 1 is appropriate in the case of the important prototype Lewis base H_2O, given that half the angle between the n-pairs in the n-pair model of H_2O should be ~54° (See Fig. 2).

It was not possible to determine experimental PE functions for $H_2O\cdots HCl$ [113] and $H_2O\cdots ClF$ [72] in same way. However, another approach was possible. The energy of each complex was obtained by carrying out a full geometry optimisation at fixed values of the out-of-plane bending coordinate ϕ in the range 0 to ~70°. The aug-cc-pVDZ/MP2 level of theory was used and correction for basis set superposition error was applied. This ab initio potential function was then fitted numerically to the expression of Eq. 1 to give the coefficients A and B and thence a and b. Once a and b were available, the matrix of the Hamiltonian $H = p_z^2/2\mu + V(z)$ was set up using a basis composed of 100 harmonic oscillator functions and was diagonalised to give the vibrational energy levels. This approach for $H_2O\cdots HF$ gave values of ϕ_{min} and the PE barrier height in good agreement with those of the experimentally determined function. Thus we can have some confidence in the results obtained when the same procedure was applied to $H_2O\cdots HCl$ [114] and $H_2O\cdots ClF$ [34]; the plots of $V(\phi)$ versus ϕ and the energy levels are displayed in Fig. 3. The equilibrium values of the angle ϕ are 45.7° and 57.4° for $H_2O\cdots HCl$ and $H_2O\cdots ClF$, respectively, and the two equivalent minima are separated by PE barriers of $V_0 = 80$ and 174 cm^{-1}, respectively. These values are similar to the experimental results 46(8)° and 126(70) cm^{-1}

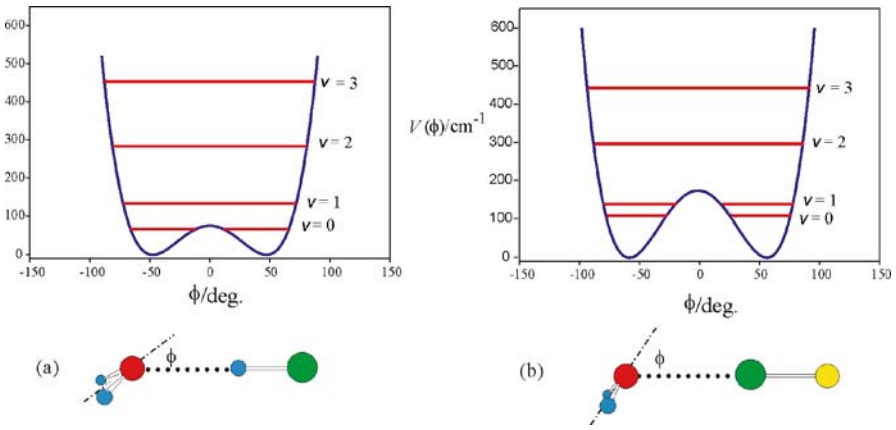

Fig. 3 The potential energy $V(\phi)$, expressed as a wavenumber, as a function of the angle ϕ for **a** $H_2O\cdots HCl$ and **b** $H_2O\cdots ClF$. These have been obtained using ab initio calculations, by the method discussed in the text. The same approach reproduces the experimental function of $H_2O\cdots HF$ (Fig. 2) very well. Several vibrational energy levels associated with the motion in ϕ are also shown. As for $H_2O\cdots HF$, the PE barrier at $\phi = 0$ is low enough that both molecules are effectively planar in the zero-point state, even though the molecules are pyramidal at equilibrium. See Fig. 1 for key to the colour coding of atoms

for $H_2O\cdots HF$ [112]. Indeed, when the zero-point rotational constants of all isotopomers investigated for each of $H_2O\cdots HCl$ or $H_2O\cdots ClF$ were fitted under the assumption of unchanged monomer geometries and collinear $O\cdots H-Cl$ and $O\cdots Cl-F$ arrangements, the results for the effective angle ϕ were 36.5(3)° and 58.9(16)°, respectively. Thus, there seems little doubt that the configuration at O in these complexes is pyramidal, a result consistent with rule 1 and the chemist's simple n-pair model of H_2O. Similar analyses have been applied with similar results to $H_2O\cdots F_2$ [34] $H_2O\cdots Cl_2$ [48], $H_2O\cdots BrCl$ [56], $H_2O\cdots Br_2$ [91] and $H_2O\cdots ICl$ [101]. In each case, the lowest vibrational energy level lies near to or above the PE maximum at the planar geometry, so the zero-point geometry is effectively planar while the equilibrium geometry is pyramidal at O. The hydrogen-bonded complexes $H_2O\cdots HX$, where X = Br [115] and I [116], are both effectively planar, but the above-described treatment is yet to be applied to give the form of the PE function.

The situation for the complexes $H_2S\cdots HX$ and $H_2S\cdots XY$ is different from that of their H_2O analogues. It has been shown by rotational spectroscopy that the conformation at S is much more steeply pyramidal, with $\phi \approx 90°$, and that there is no evidence of inversion in $H_2S\cdots HF$ [117], $H_2S\cdots HCl$ [118] or $H_2S\cdots HBr$ [119], i.e. each is permanently pyramidal at S on the time scale of the microwave experiment. Similar conclusions hold for $H_2S\cdots ClF$ [60], $H_2S\cdots BrCl$ [54], $H_2S\cdots Br_2$ [90] and $H_2S\cdots ICl$ [98]. The experimental zero-point geometries of $H_2S\cdots HCl$ and $H_2S\cdots ClF$ (derived under the assumption of unchanged monomer geometries) are compared in Fig. 4. A collinear arrangement of the $S\cdots Cl-F$ nuclei was demonstrated in the case of $H_2S\cdots ClF$ but assumed for $S\cdots H-Cl$ in $H_2S\cdots HCl$. The 90° structures seen in Fig. 4 suggest that for H_2S the n-pairs can be modelled as occupying sp hybridised valence orbitals whose axis is perpendicular to the nuclear plane, as illustrated in Fig. 4. The PE as a function of the angle ϕ for each of $H_2S\cdots HCl$ and $H_2S\cdots ClF$, as calculated[2] by the method outlined for $H_2O\cdots HCl$ and $H_2O\cdots ClF$ earlier, is shown in Fig. 5. The first few vibrational energy levels are drawn on each function. Each energy level is actually a pair having a very small separation, which indicates that the inversion motion between the two equivalent forms of each complex is very slow as a result of the relatively high PE barrier and the large separation of the two minima, in agreement with the experimental conclusion. We note that minima are at $\phi \approx \pm 90°$ in both cases, as expected from the proposed n-pair model, thereby providing evidence for the isostructural nature of pairs of hydrogen- and halogen-bonded complexes $B\cdots HCl$ and $B\cdots ClF$ when B is H_2S. For $H_2S\cdots HI$[3] and $H_2S\cdots F_2$ [35], on the other hand, there is evidence of a lower barrier to the $\phi = 0°$(planar) structure, both through the observation of vibrational satellites in the rotational

[2] Davey JB, Legon AC, unpublished calculations

[3] Legon AC, Suckley AP, unpublished observations

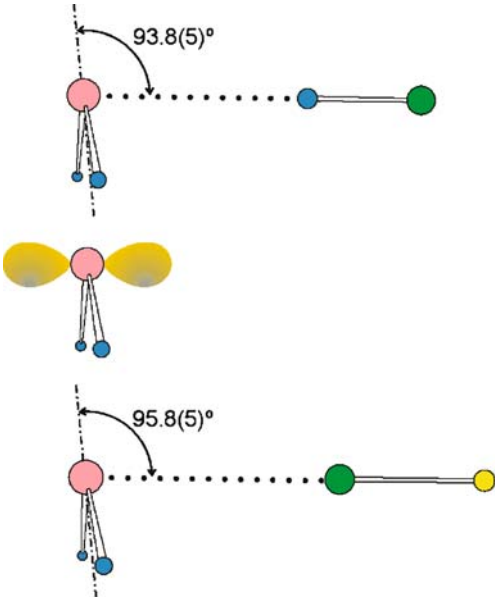

Fig. 4 The experimentally determined geometries of $H_2S\cdots HCl$ and $H_2S\cdots ClF$ drawn to scale. The n-pair model of H_2S, as discussed in the text, is shown for comparison. See Fig. 1 for key to the colour coding of atoms

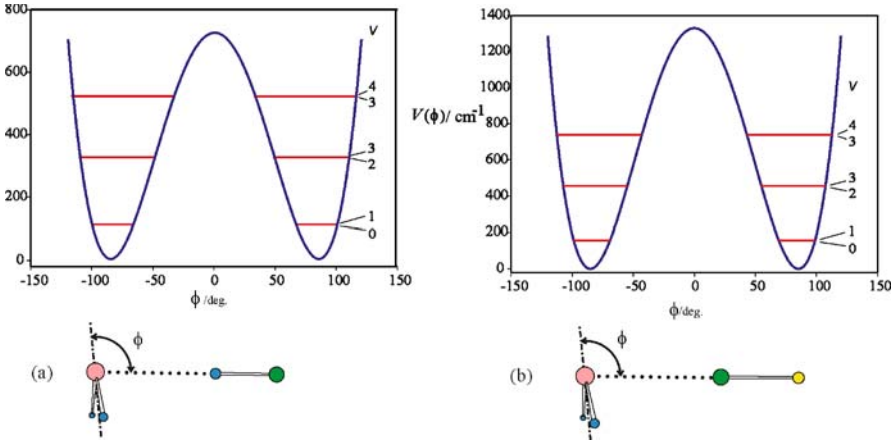

Fig. 5 The potential energy $V(\phi)$, expressed as a wavenumber, as a function of the angle ϕ for **a** $H_2S\cdots HCl$ and **b** $H_2S\cdots ClF$. These have been obtained using ab initio calculations, by the method discussed in the text. Several vibrational energy levels associated with the motion in ϕ are also shown. The PE barrier at $\phi = 0$ is high in both molecules, so that in each case the $v = 0$ and $v = 1$ vibrational energy levels are negligibly separated and hence both molecules are pyramidal in the zero-point state and at equilibrium. The values of ϕ_e and the effective values ϕ_0 determined experimentally (see Fig. 4) are in good agreement. See Fig. 1 for key to the colour coding of atoms

spectra and the angle ϕ determined by fitting rotational constants. This observation can be readily rationalised when we note that, in general, complexes B···F_2 and B···HI are more weakly bound for a given B than those involving other HX or XY molecules.

3.1.2.2 Non-linear Halogen Bonds and Hydrogen Bonds

The ab initio calculations for $H_2Z\cdots HCl$ and $H_2Z\cdots ClF$, where Z is O or S, (referred to in Sect. 3.1.2.1) reveal that the nuclei Z···H – Cl and Z···Cl – F deviate insignificantly from collinearity. For example, the angular deviations θ are less than 2° in $H_2O\cdots F_2$, $H_2O\cdots ClF$ and $H_2O\cdots HCl$ [34, 114]. Is this always the case and, if not, can the deviation from a linear arrangement be measured experimentally?

The position of the subunit HX in the principal inertia axes system of an effectively planar complex $H_2O\cdots HX$ is difficult to determine from zero-point rotational constants because of the large amplitude motion of the H_2O and HX subunits, which involves mainly the H atoms, and the small contributions that the H atoms make to the principal moments of inertia. If H_2O is replaced by the cyclic ether oxirane, $(CH_2)_2O$, to yield the complex $(CH_2)_2O\cdots HX$, the inversion motion is quenched and the complex has a pyramidal configuration at O and C_S symmetry, even in the zero-point state [120]. This allows the orientation of the oxirane subunit in the principal inertia axis system of the complex to be established. Moreover, if the atom X has a quadrupolar nucleus, determination of the complete nuclear quadrupole coupling tensor $\chi_{\alpha\beta}(X)$ of X from the rotational spectrum of the complex gives the orientation of HX in the principal inertia axis system. If *a* is the principal inertia axis (which passes almost through the centre of the oxirane ring and close to the centre of mass of the HX subunit), *ab* is the molecular symmetry plane and *z* the HX internuclear axis, it can be shown [28, 29] that the angle α_{az} between *a* and *z* is given in terms of the elements of $\chi_{\alpha\beta}(X)$ by the expression:

$$\alpha_{az} = \tan^{-1}\left(\frac{-\chi_{ab}}{\chi_{aa} - \chi_{bb}}\right). \tag{3}$$

Of primary interest here is the important result that α_{az} so obtained is independent of the large amplitude, zero-point angular oscillation of the HX subunit even when components of the zero-point coupling tensor are used in Eq. 3. The assumptions made in deriving Eq. 3 are that the electric field gradient at X is unperturbed on complex formation and that the effect of the intermolecular stretching motion on the coupling tensor is negligible. Once α_{az} is available, the principal moments of inertia of sufficient isotopomers of, for example, $(CH_2)_2O\cdots HCl$ can be fitted under the constraint that the result-

ing structure must also reproduce this angle. The geometry of $(CH_2)_2O\cdots HCl$ so obtained [28, 120] is shown in Fig. 6.

The angle θ defines the non-linearity of the hydrogen bond and ϕ is the angle O–H–Cl, as indicated. Also shown in Fig. 6 is the geometry similarly determined for the halogen-bond analogue of $(CH_2)_2O\cdots HCl$, namely $(CH_2)_2O\cdots ClF$ [67]. We note immediately a striking similarity between the angles ϕ of these two complexes [69.1(1)° and 67.3(1)°, respectively], a result that can be understood on the basis of rule 1 if the oxygen atom of oxirane carries two equivalent n-pairs, as drawn schematically in Fig. 6. By contrast, there is a significant difference in the non-linearities [θ = 16.5(1)° and 2.9(1)°] of the hydrogen bond $O\cdots H-Cl$ and the halogen bond $O\cdots Cl-F$ in the two complexes. We shall see that this relationship between $(CH_2)_2O\cdots HCl$ and $(CH_2)_2O\cdots ClF$ is an example of a common property of the two series $B\cdots HCl$ and $B\cdots ClF$ and, moreover, that the propensity to be non-linear is an important characteristic of the hydrogen bond.

Other Lewis bases in which the electron donor atom Z carries two equivalent n-pairs and which form complexes of C_S symmetry with HCl and ClF have been investigated by the same approach. The resulting geometries when B is formaldehyde are shown, together with the conventional n-pair model of CH_2O, in Fig. 7. The angle ϕ is virtually identical in $H_2CO\cdots HCl$ [121] and $H_2CO\cdots ClF$ [79] and is close to that expected from the n-pair model in which the angle between the n-pairs is ∼120°. The hydrogen bond again deviates significantly from linearity [θ = 20.3(8)°] but the $O\cdots Cl-F$ system is essentially collinear [θ = 3.2(7)°].

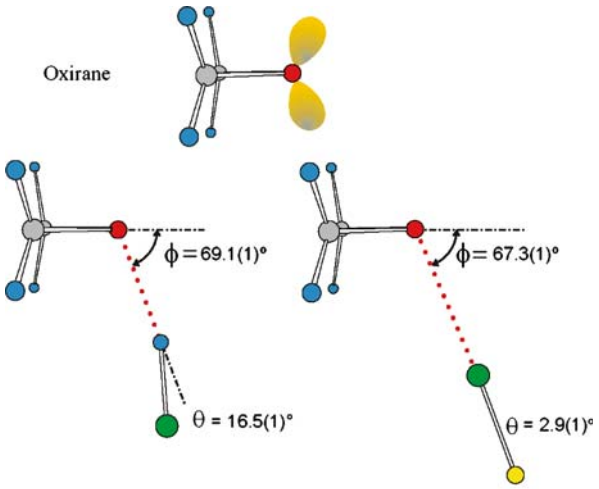

Fig. 6 The experimentally determined geometries of oxirane···HCl and oxirane···ClF drawn to scale. The n-pair model of oxirane is shown for comparison. While the angle ϕ is similar in both complexes, the non-linearity θ of the hydrogen bond is much greater than that of the halogen bond. See Fig. 1 for key to the colour coding of atoms

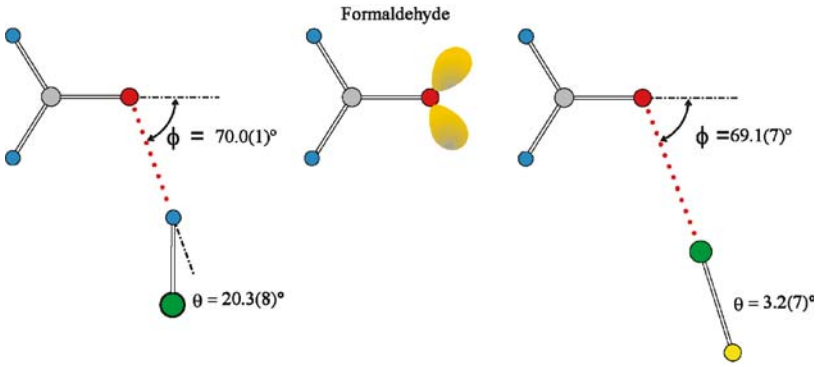

Fig. 7 The experimentally determined geometries of $CH_2O\cdots HCl$ and $CH_2O\cdots ClF$, drawn to scale, are shown in comparison to the n-pair model of formaldehyde. The angle ϕ is again similar in both complexes but the non-linearity θ of the hydrogen bond is much greater than that of the halogen bond. See Fig. 1 for key to the colour coding of atoms

It is possible to test the n-pair model more precisely when O is the electron donor atom. In the series of cyclic ethers oxirane $[(CH_2)_2O]$, oxetane $[(CH_2)_3O]$, and 2,5-dihydrofuran $[(CHCH_2)_2O]$, the internal ring angle COC increases from ∼60° through ∼90° to ∼109° (the tetrahedral angle). It is generally accepted that this increase is accompanied by a corresponding decrease in the angle between the n-pairs carried by O; if so the angle ϕ should decrease correspondingly. The n-pair models of these three Lewis bases are shown in Fig. 8 together with the observed geometries of their complexes with HCl. Table 1 gives the angles ϕ and θ for the two series $B\cdots HCl$ and $B\cdots ClF$, where B is oxirane [67, 120], oxetane [122] or 2,5-dihydrofuran [29, 77], all determined from their rotational spectra under assumptions identical to those described earlier for the oxirane complexes [$(CH_2)_3O\cdots ClF$ has not yet been investigated].

It is clear from Fig. 8 and Table 1 that the angle ϕ does indeed decrease as expected if the n-pair models and rule 1 were applicable. Moreover, the hydrogen bond non-linearity θ decreases along the series B = oxirane, oxetane, 2,5-dihydrofuran. On the other hand, the values of θ for oxirane$\cdots ClF$ and 2,5-dihydrofuran$\cdots ClF$ (included in Fig. 8) reveal that the halogen bond shows little propensity to be non-linear.

Oxirane is an important Lewis base in the present context. The O atom carries two equivalent n-pairs of electrons, as it does in H_2O, but oxirane has the advantage over water in that it is possible to determine both angles ϕ and θ for its complexes with HCl and ClF because the non-zero off-diagonal element χ_{ab}(Cl) of the Cl nuclear quadrupole coupling tensor is available. The corresponding Lewis base in which an S atom carries two equivalent n-pairs is thiirane. Each of the pair of complexes $(CH_2)_2S\cdots HCl$ and $(CH_2)_2S\cdots ClF$ has C_S symmetry and here it is the off-diagonal element χ_{ac}(Cl) that is non-zero

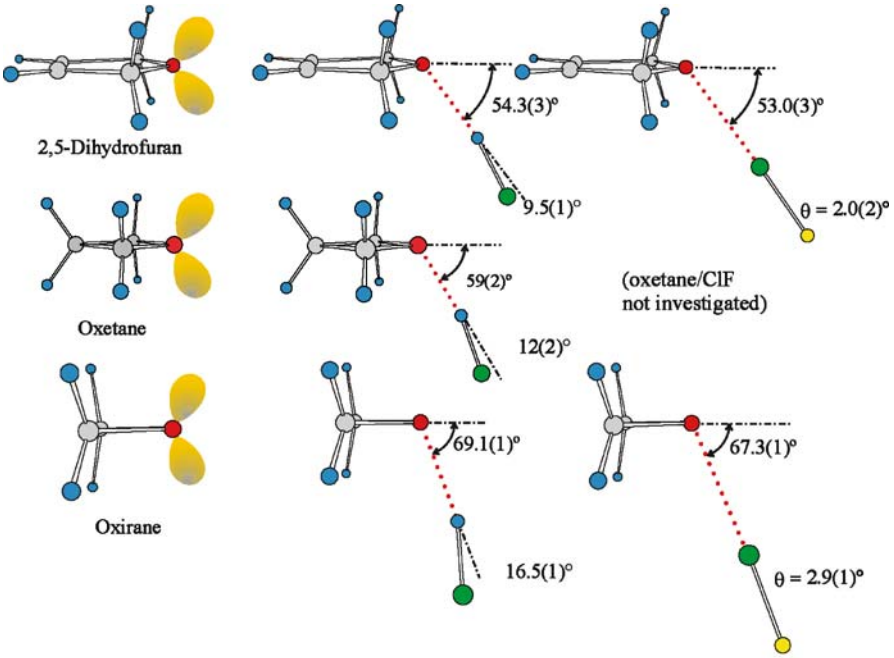

Fig. 8 The n-pair models of 2,5-dihydrofuran, oxetane and oxirane (*first column*) and the experimental geometries of their complexes with HCl (*second column*) and ClF (*third column*), each drawn to scale. The angle ϕ is almost identical in B···HCl and B···ClF for a given B but increases from 2,5-dihydrofuran, through oxetane, to oxirane, as expected from the model (see text). The non-linearity of the hydrogen bond increases monotonically from 2,5-dihydrofuran to oxirane. See Fig. 1 for key to the colour coding of atoms

Table 1 The angles ϕ and θ (in degrees; see Fig. 8 for definitions) in complexes B···HCl and B···ClF, where B is one of the cyclic ethers 2,5-dihydrofuran, oxetane or oxirane

B	B···HCl		B···ClF	
	ϕ	θ	ϕ	θ
Oxirane	69.1(1)	16.5(1)	67.3(1)	2.9(1)
Oxetane	59(2)	12(2)	···	···
2,5-Dihydrofuran	54.3(3)	9.5(1)	53.0(3)	2.0(2)

because the axis *a* and *c* lie in the molecular symmetry plane. Thus both ϕ and θ can be determined for each complex, in contrast to the position for the H_2S analogues, for which only in $H_2S\cdots ClF$ was it possible to establish the collinearity of the $S\cdots Cl-F$ nuclei. The determined geometries (drawn to scale) of $(CH_2)_2S\cdots HCl$ [28, 123] and $(CH_2)_2S\cdots ClF$ [69] are displayed in Fig. 9.

The values of ϕ are both close to 90°, which suggests an n-pair model of thiirane (see Fig. 9) similar to that described for H_2S earlier. A reason for the

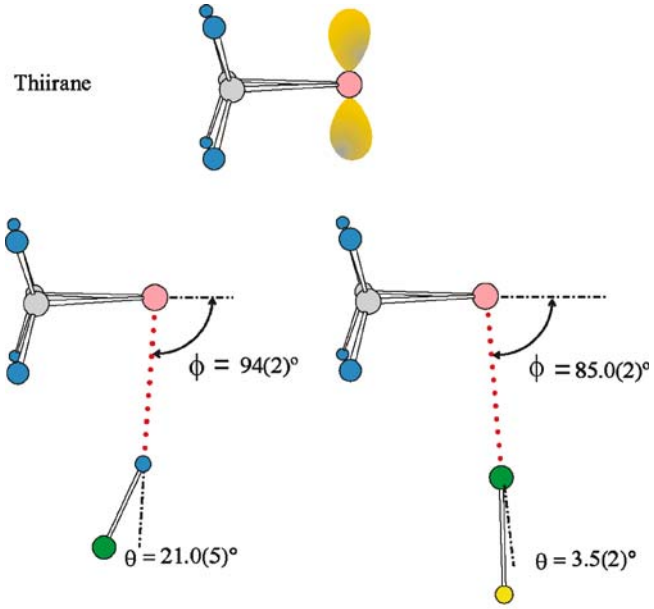

Fig. 9 The experimentally determined geometries of thiirane···HCl and thiirane···ClF drawn to scale. The n-pair model of thiirane is shown for comparison. The angle ϕ is slightly different in the two complexes for reasons discussed in [69]. The non-linearity θ of the hydrogen bond is again greater than that of the halogen bond. See Fig. 1 for key to the colour coding of atoms

slightly smaller angle in the case of $(CH_2)_2S\cdots ClF$ is discussed in [69]. It is clear that the hydrogen bond in $(CH_2)_2S\cdots HCl$ deviates significantly from linearity [$\phi = 21.0(5)°$] while the halogen bond in $(CH_2)_2S\cdots ClF$ is close to linear[$\phi = 3.5(2)°$]. The hydrogen bonds in the complexes $(CH_2)_2S\cdots HF$ [124] and $(CH_2)_2S\cdots HBr$ [28, 125] are also significantly non-linear.

3.1.3 B Carries Two Inequivalent n-Pairs

Sulfur dioxide is an example of a simple Lewis base that carries two sets of inequivalent n-pairs, one set on each O atom. The n-pair model (in which the π bonding pairs are not drawn and are ignored here) is shown in Fig. 10. The geometries of $SO_2\cdots HF$ [126, 127], $SO_2\cdots HCl$ [28, 126] and $SO_2\cdots ClF$ [70] have all been determined from investigations of their rotational spectra. Each molecule is planar and belongs to the C_S point group. Scale drawings for $SO_2\cdots HCl$ and $SO_2\cdots ClF$ are displayed in Fig. 10.

We note that the HCl and ClF molecules attach, approximately at least, along the axis of the *cis* n-pair, as required by rule 1, with angles ϕ of 143.0(1)° and 131.9(6)°, respectively, although the former value may be influenced by

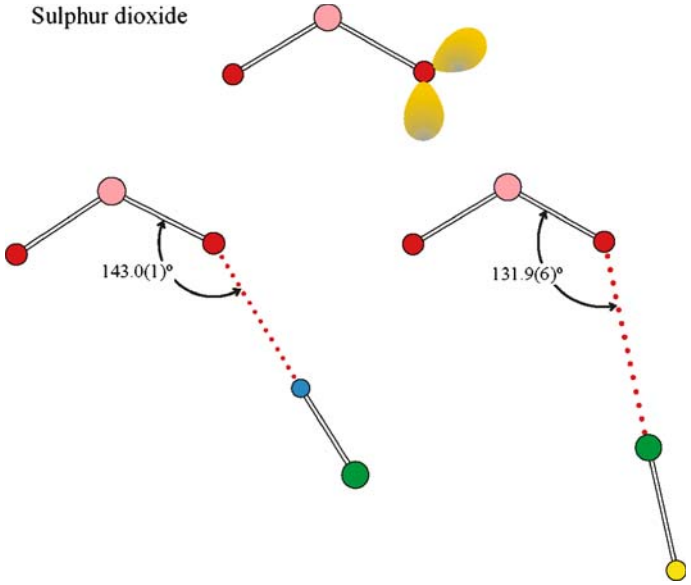

Fig. 10 The n-pair model of sulfur dioxide and the experimental geometries of $SO_2\cdots HCl$ and $SO_2\cdots ClF$. Note that neither the hydrogen bond nor the halogen bond deviate significantly from linearity. See Fig. 1 for key to the colour coding of atoms

the non-rigid behaviour noted in $SO_2\cdots H-Cl$. The hydrogen bond and the chlorine bond are both nearly linear [$\theta = -2.5(7)^\circ$ and $-0.7(2)^\circ$, respectively], a result which is different from those obtained for other B···HCl and B···ClF pairs belonging to the C_S point group. This will be discussed when the rules for rationalising the geometries of hydrogen- and halogen-bonded complexes are refined in Sect. 6.

3.2 Angular Geometries of B···ClF and B···HCl in Which B is a π-Pair Donor

According to the rules for predicting angular geometries of hydrogen-bonded complexes B···HX, given earlier, the HX molecule lies along the local symmetry axis of a π orbital when B carries no non-bonding electron pairs and only π pairs. In this section, we examine whether this rule also applies to halogen-bonded complexes B···XY. We consider first Lewis bases that offer only a single π pair.

3.2.1 B Carries a Single-π-Pair

The experimentally determined geometries of the complexes of the simplest π electron donor, ethene, with HCl [128] and ClF [65] are displayed in Fig. 11.

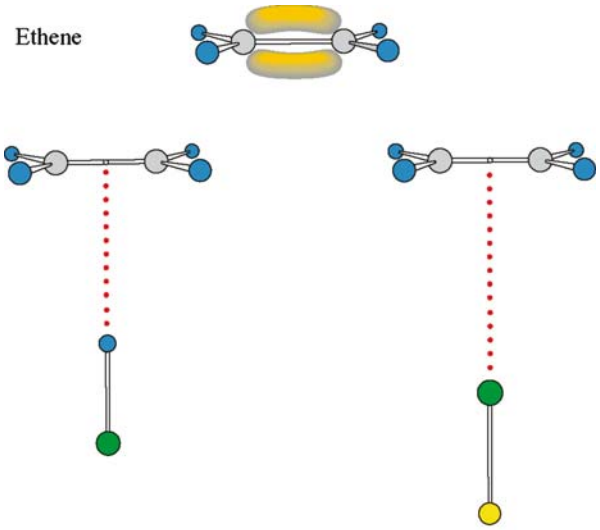

Fig. 11 The experimental geometries of ethene···HCl and ethene···ClF (drawn to scale) and the π-electron model of ethene. See Fig. 1 for key to the colour coding of atoms

These two molecules are clearly isostructural and of C_{2v} symmetry, with the XY or HX molecule lying along the C_2 axis of ethene that is perpendicular to the plane containing the C_2H_4 nuclei. Other complexes ethene···XY, where XY = Cl_2 [46], BrCl [51], Br_2 [89] and ICl [96], and other complexes ethene···HX, where X is F [129] or Br [130], have also been shown to have the form illustrated in Fig. 11. It is of interest to note that C_2H_4···Cl_2 was detected through its UV spectrum many years ago [131] and that the pre-reactive complex C_2H_4···Br_2 has recently been shown to be important on the overall reaction coordinate for bromination through autocatalytic action of bromine [132].

Each angular geometry can be rationalised on the basis of rule 2 (see earlier) with the aid of the familiar π bonding electron density distribution of ethene, which is included in Fig. 11. In all cases, the electron acceptor molecule XY or HX lies along the symmetry axis of the π orbital of the Lewis base. The electrophilic end, $^{\delta+}$X of XY or $^{\delta+}$H of HX, as appropriate, interacts with the π-electron density. There is no evidence that the hydrogen bonds or the halogen bonds in these complexes are not strictly linear in the equilibrium geometry (i.e. that the arrangements ∗···H–X or ∗···X–Y are not collinear, where ∗ is the midpoint of the C – C bond). In view of the symmetry of ethene, non-linear hydrogen or halogen bonds are not expected.

Ethyne has two π bonding orbitals at right angles to each other and a resultant π electron density that is cylindrically symmetric with respect to the internuclear axis. Complexes of ethyne with HF [133], HCl [134], HBr [135], ClF [66], Cl_2 [47], BrCl [50], Br_2 [92] and ICl [95] have been characterised by

rotational spectroscopy. Each complex has the planar, T-shaped geometry of C_{2v} symmetry that is predicted by applying rule 2 using the π-bonding model of ethyne.

3.2.2 B Carries Pseudo-π-Pairs

Cyclopropane resembles an alkene in its chemical behaviour. This fact led Coulson and Moffitt [136] to propose a model for cyclopropane in which a pseudo-π carbon–carbon bond is formed by overlap of a pair of sp^3 hybrid orbitals on adjacent carbon atoms. A schematic diagram showing the electron density distribution between a pair of C atoms in cyclopropane resulting from such a model is shown in Fig. 12. The symmetry axis of the pseudo-π orbital coincides with a median of the cyclopropane equilateral triangle. Hence, according to rule 2, the angular geometry of cyclopropane···ClF [73], or of cyclopropane···HCl [137], is predicted to have C_{2v} symmetry, with ClF, or HCl, lying along the extension of the median. The electrophilic end $^{\delta+}$Cl of ClF, or $^{\delta+}$H of HCl, is expected to interact with the pseudo-π electron dens-

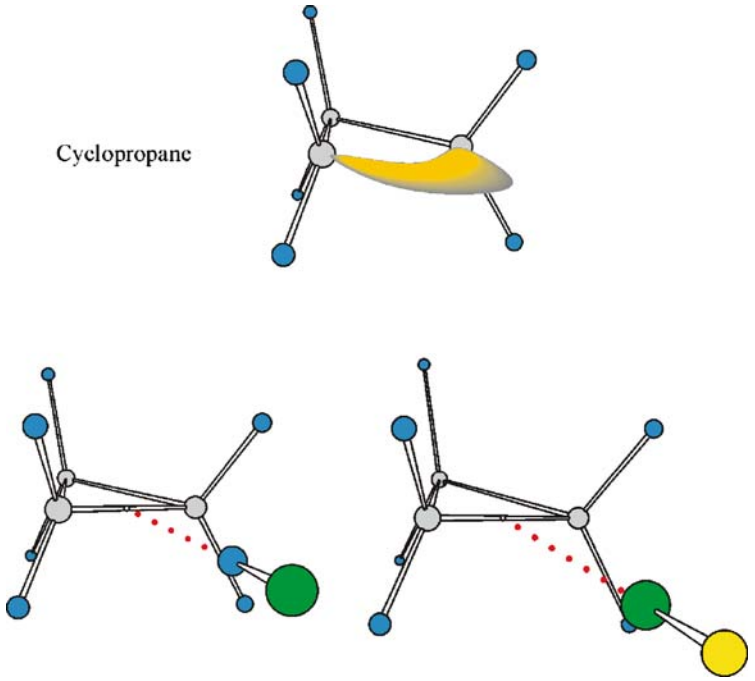

Fig. 12 The experimental geometries of cyclopropane···HCl and cyclopropane···ClF (drawn to scale) and the Coulson–Moffitt pseudo-π-electron model of cyclopropane. See Fig. 1 for key to the colour coding of atoms

ity of the C – C bond in preference to $F^{\delta-}$ or $Cl^{\delta-}$, respectively. The observed geometries of the two complexes, included in Fig. 12, are clearly as predicted by rule 2. Cyclopropane···HF has a similar angular geometry [138].

3.2.3
B Carries Several-π-Pairs

Rule 2 can also be tested when the Lewis base B carries no n-pairs but two or more π-electron pairs, either conjugated or cumulative. Strictly, cyclopropane might be considered in this category but has been discussed in Sect. 3.2.2 as the prototype of a pseudo-π donor for convenience.

3.2.3.1
B is a Conjugated π-bonded System

trans-1,3-Butadiene is the prototype Lewis base offering a pair of conjugated, but non-aromatic, π bonds as electron donors. According to rule 2, the axis of a ClF or HCl molecule, for example, should lie along the local symmetry axis of one of the π-orbitals in the equilibrium geometry of a complex with *trans*-1,3-butadiene. There will be four equivalent geometries because there are two equivalent π orbitals and either may be approached from above or below the molecular plane. Two possibilities then exist, however. If the potential energy barriers to tunnelling between the four equivalent positions are sufficiently high, the ClF/HCl molecule will be localised at one of the π bonds. On the other hand, if the PE barriers are low enough, the diatomic molecule might tunnel quantum mechanically through them and sample the four equivalent positions. The geometry of the 1,3-butadiene···ClF complex, as determined from its ground-state rotational spectrum [76], is shown, drawn to scale, in Fig. 13. There was no evidence from the observed spectrum of tunnelling between the equivalent structures and therefore it was concluded that the ClF molecule is localised at one site. The geometry displayed in Fig. 13 is consistent with rule 2. Thus, the ClF axis lies perpendicular to the plane of the nuclei in 1,3-butadiene and the angle ϕ ($\angle C_2 - * \cdots Cl$) is 95°, where $*$ is the mid-point of a terminal C – C bond. The rotational spectrum of 1,3-butadiene···HCl exhibits the characteristics of non-rigid-rotor behaviour, probably as a result of a low potential energy barrier between equivalent conformers[4], but the analysis is incomplete and therefore comparison of the geometries of the ClF and HCl complexes with 1,3-butadiene is unavailable.

Benzene is the prototype aromatic Lewis base. It offers formally three pairs of equivalent, conjugated π bonds as the potential electron donor. Symmetric-top-type rotational spectra have been observed for the benzene···HX complexes, where X is F [139], Cl [140] or Br [141], by methods (molecular-beam

[4] Kisiel Z, Legon AC, unpublished observations

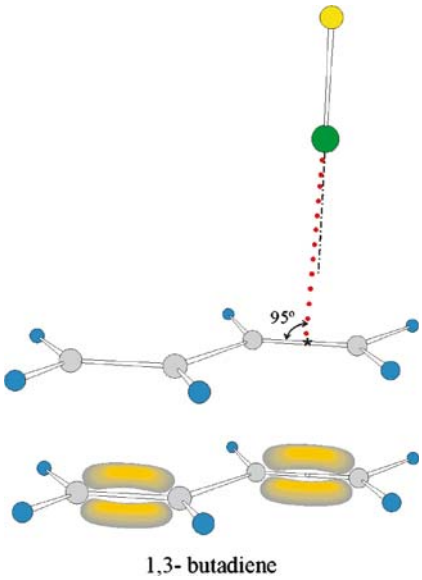

Fig. 13 The experimental geometry of 1,3-butadiene···ClF drawn to scale and the π-electron model of 1,3-butadiene. The geometry of 1,3-butadiene···HCl is not yet available for comparison. See Fig. 1 for key to the colour coding of atoms

electric resonance spectroscopy and pulsed-jet, Fourier-transform microwave spectroscopy) involving supersonic expansion of gas mixtures of benzene and HX in argon. In each case, only information about the vibrational ground state is available. Benzene···ClF also has a symmetric top-type spectrum but exhibits evidence of non-rigid-rotor behaviour [80]. The ground-state spectrum is accompanied by a single vibrational satellite spectrum which is presumably associated with a low-energy vibrationally excited state, given the low effective temperature of the experiment. A possible interpretation of these observations for benzene···ClF is that the geometry of the complex is as shown in Fig. 14, that is, in the zero-point state, the ClF subunit executes the motion defined by the angle ϕ, with a PE maximum at the $C_{6v}(\phi = 0°)$ conformation. Thus, the electrophilic end $^{\delta+}$Cl of the ClF subunit interacts with the π-electron density as it traces out the nearly circular path in the ϕ coordinate, as indicated, encompassing the six carbon atoms. This path presumably corresponds to a potential energy minimum relative to a maximum at the $C_{6v}(\phi = 0°)$ conformation but is itself likely to present small maxima at the carbon atoms.

It is possible that the complexes benzene···HX can be described in a similar way, but in the absence of any observed non-rigid-rotor behaviour or a vibrational satellite spectrum, it is not possible to distinguish between a strictly C_{6v} equilibrium geometry and one of the type observed for benzene···ClF. In either case, the vibrational wavefunctions will have C_{6v} symmetry, however.

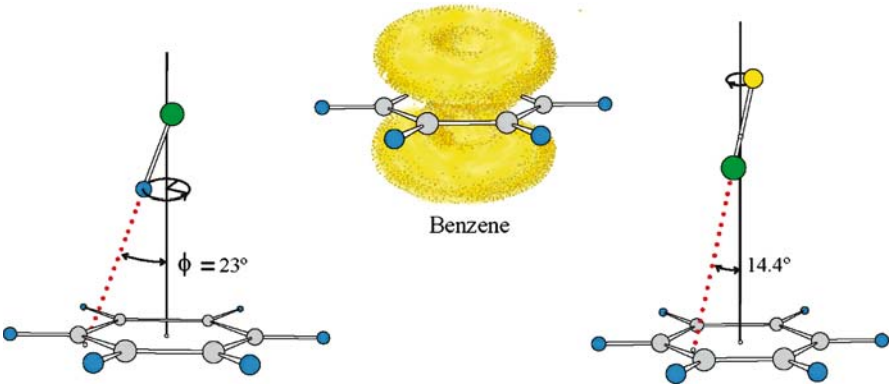

Fig. 14 The experimental geometries of benzene···HCl and benzene···ClF (to scale) and the π-electron model of benzene. See text for discussion of the motion of the ClF subunit, as inferred from an analysis of the rotational spectrum of benzene···ClF. See Fig. 1 for key to the colour coding of atoms

3.2.3.2
B is a Cumulative π-Bonded System

The π-electron density model of allene, the prototype of molecules that carry two cumulative π bonds, is shown in Fig. 15. According to rule 2, complexes of allene with either HCl or ClF should have the diatomic subunit lying along an axis that passes through, or close to, the midpoint of one of the C – C bonds and is perpendicular to the plane formed by the two C atoms involved and the two H atoms attached to one of them. The geometries of allene···HCl[5] and allene···ClF [75], as determined by means of their rotational spectra, are included in Fig. 15. The angle of rotation ψ about the C = C = C axis cannot be determined spectroscopically because allene is a symmetric-top molecule. The angle ψ would be 0° if, as seems likely, the electrophilic end $^{\delta+}$H of HCl or $^{\delta+}$Cl of ClF interacts with the maximum of π electron density, but $\psi = 90°$ would require that HCl or ClF lies in the nodal plane of the π orbital. Hence, the angle ψ was set to zero. It is possible to determine both the angles θ and ϕ for these molecules of C_S symmetry by the methods outlined in Sect. 3.1.2.2 because the off-diagonal element χ_{ab} of the Cl nuclear quadrupole coupling tensor is non-zero and determinable. We note from Fig. 15 that the angle ϕ for each complex is close to the value of 90°, as required by rule 2. The non-linearity is $\theta \approx 7°$ for the hydrogen bond in allene···HCl[6] and $\theta = 4.9(15)°$ [75] for the halogen bond in allene···ClF. Both these observations indicate only a minor secondary interaction of $^{\delta-}$Cl and $^{\delta-}$F, respectively, with the nearest H atom on the C atom

[5] Fillery-Travis AJ, Legon AC, unpublished observations
[6] Fillery-Travis AJ, Legon AC, unpublished observations

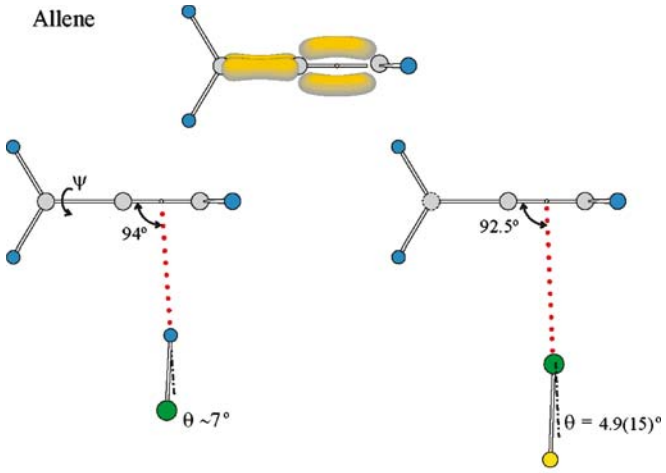

Fig. 15 The experimental geometries of allene···HCl and allene···ClF, drawn to scale. The π-electron model for allene is also shown. The angles $C_2{-}{*}\cdots H$ and $C_2{-}{*}\cdots Cl$, respectively, where $*$ is the centre of the C – C bond, are both close to 90°, as required by rule 2. The hydrogen and halogen bonds both show small non-linearities. See Fig. 1 for key to the colour coding of atoms

remote from the primary interaction. Allene···HF exhibits a similar geometry [142].

3.2.3.3
B Carries Both-π- and Pseudo-π-Pairs

Methylenecyclopropane has two pseudo-π C – C bonds of its cyclopropane ring adjacent to the π bond between C_1 and C_2. It is therefore the prototype for a Lewis base that offers cumulative π and pseudo-π-bonds in competition as electron donors. The observed geometries of complexes of methylenecyclopropane with ClF [78] and HCl [143], as determined from spectroscopic constants obtained by analysis of rotational spectra, are shown in Fig. 16. Each has C_S symmetry, with the *ab* principal inertia plane coincident with the plane of symmetry. Accordingly, the off-diagonal element χ_{ab}(Cl) of the Cl nuclear quadrupole coupling tensor was found to be non-zero and was accurately measured in each case. By applying the approach set out in Sect. 3.1.2.2, it was possible to determine both the angles ϕ and θ, as defined in Fig. 16. The hydrogen and halogen bonds clearly involve the interaction of $^{\delta+}$H and $^{\delta+}$Cl, respectively, with the $C_1 - C_2$ π bond rather than with a pseudo-π bond of the cyclopropane ring. Moreover, the angles ϕ are close to 90° in both complexes, as would be predicted from rule 2, but we note that while the hydrogen bond is significantly non-linear [$\theta = 17.5(2)°$] the halogen bond is much less so [$\theta = 4.9(1)°$]. It is now established for several such pairs of complexes of C_S

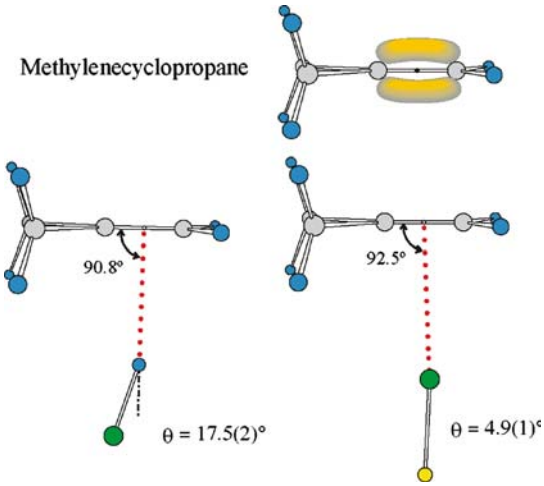

Fig. 16 The experimental geometries of methylenecyclopropane···HCl and methylenecyclopropane···ClF, drawn to scale. The π-electron model for the Lewis base is also shown. The angles C–∗···H and C–∗···Cl, respectively, where ∗ is the centre of the C – C double bond, are both close to 90°, as required by rule 2. The halogen bond again exhibits a smaller non-linearity θ than the hydrogen bond. See Fig. 1 for key to the colour coding of atoms

symmetry that the hydrogen bond is significantly non-linear while the corresponding halogen bond is not. We shall return later (Sect. 6) to this important difference between the two types of intermolecular bond. Other complexes of methylenecyclopropane with HX (X = F [144] and Br [145]) have geometries similar to that for X = Cl.

3.3 Angular Geometries of B···ClF and B···HCl in Which B is a Mixed n-Pair/π-Pair Donor

According to rule 3, if a Lewis base B carries both non-bonding and π-bonding electron pairs, the n-pairs are definitive of the angular geometry. There are many examples of simple Lewis bases B that can in principle act as either n- or π-electron pair donors. These include CO, HCN, H_2CO, furan, thiophene, pyridine, etc. We note that, for convenience, we considered H_2CO earlier as an example of a Lewis base carrying a pair of equivalent n-pairs and ignored the π pair. In fact, H_2CO···HCl [121] and H_2CO···ClF [79] are examples that obey rule 3. The complexes HX with carbon monoxide when X = F [146], Cl [147], Br [148], and I [149] have all been investigated through their rotational spectra. Each is linear, with the order of the atoms OC···HX in the lowest energy conformer, so that the n-pair on the C atom takes precedence over the π pairs (and indeed the n-pair on O), as predicted by rule 3.

Likewise, the complexes of CO with the dihalogen molecules XY = ClF, [61] Cl_2, [39], BrCl [49], Br_2 [87] and ICl [94] are all linear in their equilibrium geometries with atoms in the order OC···XY and with X as the more electropositive halogen atom when XY is a heteronuclear dihalogen. Thus, the n-pair carried by C again defines the angular geometry in preference to the π pair. Complexes of the type N_2···HX, where X = F [150], Cl [151, 152] and Br [153] are all linear, as are N_2···XY, where XY is ClF [71], BrCl [58] and ICl [100]. Thus the complexes of N_2 also obey rule 3. The same pattern emerges for the series of complexes formed by hydrogen cyanide with hydrogen halide molecules and with dihalogen molecules. Thus, each complex has been shown to have a linear equilibrium geometry, with atoms in the order HCN···HX, when X = F [154, 155], Cl, [156], Br [157] or I [158], or HCN···XY, when XY = F_2 [32], ClF [64],Cl_2 [41], BrCl [53] or ICl [99]. Again, when XY is a heteronuclear dihalogen, X is always the more electropositive atom. Those members of the two series CH_3CN···HX and CH_3CN···XY so far investigated (namely HX = HF [159, 160] and HCl [161] and XY = F_2 [31] and ClF [84]) indicate that the same conclusion appears to hold when methyl cyanide is the electron donor. So, there is ample evidence that rule 3 holds for both hydrogen- and halogen-bonded complexes.

Is there any evidence that this rule can be contravened? To answer this question, the complexes of vinyl fluoride, furan and thiophene with HCl and ClF will be considered. Vinyl fluoride, CH_2CHF, is an example of a mixed n-pair/π-pair donor in which, unlike CO, HCN, CH_3CN or CH_2O, the pairs of electrons (a π-pair shared between C_1 and C_2 and an n-pair on F) do not have an atom in common. In addition, its complexes with HCl and ClF are important in the context of linear/non-linear hydrogen and halogen bonds. On the other hand, furan and thiophene are examples of mixed n-pair/π-pair aromatic donors in which the n-pair can be withdrawn into the ring.

The geometries of complexes CH_2CHF···HCl [85, 162] and CH_2CHF···ClF [85], as determined from their ground-state spectroscopic constants, are displayed in Fig. 17. Each complex is effectively planar and we note that in each case the F atom of vinyl fluoride acts as the electron donor. The simple electron density model showing the three n-pairs on F (see Fig. 17) leads to the prediction of a value of ∼115° for the angles C – F···H and C – F···Cl in CH_2CHF···HCl and CH_2CHF···ClF, respectively. The observed values ϕ = 123.7(1)° and 125.7(3)°, respectively, are very similar and reasonably close to 115°. This indicates that rule 3 is again obeyed. The angular deviations of the F···H – Cl nuclei and the F···Cl – F nuclei from a collinear arrangement (defined as θ in Fig. 17) are different, however. As is the case for several complexes of C_S symmetry discussed earlier, the halogen bond is strictly linear [θ = 0.6(1)°] while the hydrogen bond deviates by θ = 18.3(1)° from linearity. The complexes vinyl fluoride···HF [163] and vinyl fluoride···HBr [164] are isostructural with vinyl fluoride···HCl and exhibit similarly non-linear hydrogen bonds.

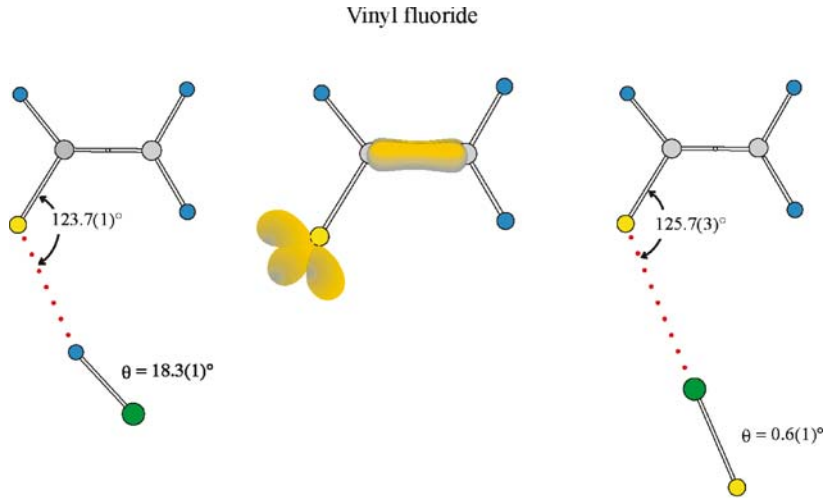

Fig. 17 The n-pair/π-pair model of vinyl fluoride and scale drawings of the experimental geometries of vinyl fluoride···HCl and vinyl fluoride···ClF. Note that rule 3 is obeyed, with the n-pair taking precedence over the π-pair in defining the angular geometry in both cases. The angles C_1–F···H and C_1–F···Cl of the HCl and ClF complexes, respectively, are similar, but the non-linearity of the hydrogen bond is large compared with that of the halogen bond, which is negligible. See Fig. 1 for key to the colour coding of atoms

Furan is the prototype of molecules that carry both non-bonding and aromatic π bonding electron pairs. The usual model for the n-pair and π electron density in this molecule is shown in Fig. 18. The oxygen atom is taken to have a non-bonding electron pair in an orbital whose symmetry axis coincides with the C_2 axis of furan.

If rule 3 is applied to complexes of furan with HCl or ClF, the predicted geometry would be one that retains C_{2v} symmetry, with the HCl or ClF molecule lying along the axis of the n-pair, and hence along the furan C_2 axis, with $^{\delta+}$H or $^{\delta+}$Cl, respectively, nearest to O. The experimentally determined geometry of furan···HCl [165], which is shown in Fig. 18, is indeed precisely as predicted, as is that of furan···HF [166]. The geometry of furan···ClF [81], established by rotational spectroscopy, is strikingly different, as may be seen from Fig. 18. It is obviously not the analogue of that obtained for furan···HCl. Instead, the end $^{\delta+}$Cl of ClF appears to interact with the π electron density associated with carbon atoms C_2 and C_3, so that this geometry violates rule 3. When furan was replaced by its sulfur analogue thiophene, *both* thiophene···HCl [167] and thiophene···ClF [83] were shown to posses a face-on geometry and both violate rule 3. Thiophene···HF [168] and thiophene···HBr [169] have face-on geometries similar to that of thiophene···HCl.

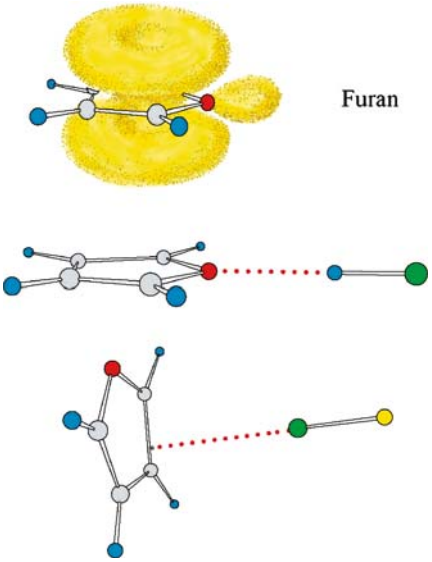

Fig. 18 The n-pair/π-pair model of furan together with the experimental geometries of furan···HCl and furan···ClF. Furan···HCl, which has a planar geometry of C_{2v} symmetry with HCl lying along the C_2 axis, clearly obeys rule 3 but the observed face-on arrangement for furan···ClF demonstrates that rule 3 is violated in this case. See Fig. 1 for key to the colour coding of atoms

The behaviour of the n-pair/aromatic π-pair donors can be understood by considering the electric charge distributions for the series of heterocyclic molecules pyridine, furan and thiophene. A convenient tabulation of the molecular electric dipole and quadrupole moments of these compounds is given in ref. [19]. The electric dipole moment decreases along the series, an observation which has been interpreted as indicating a progressive withdrawal of the n-pair on the heteroatom into the ring. On the other hand, the magnitude of out-of-plane component, Q_{cc}, of the electric quadrupole moment, which is a measure of the extension of the π cloud above and below the molecular plane, increases along this series. Thus, thiophene is the member of the series most likely to violate rule 3 and pyridine the least likely. Certainly, both the HCl and ClF complexes of thiophene are of the π-type. The complexes pyridine···HX, for X = F [170], Cl [171] and Br [172] are all of the n-type, with HX lying along the C_2 axis and forming a strong hydrogen bond to the heteroatom. Furan is the intermediate case and whether the n- or π-electron pairs define the geometry of the complex is evidently sensitive to the precise nature of the electron acceptor. Thus, furan···HCl is an n-pair complex while furan···ClF has a π-type interaction. Interestingly, furan···HBr [173] also has the face-on conformation, so there is a changeover between X = Cl and Br in the furan complexes.

3.4
Radial Geometries of Complexes B···XY and B···HX: A Summary

Radial geometries of B···XY and B···HX are also systematically related. Only a summary will be given here; the reader is referred to earlier publications for detailed discussion [19, 174–178].

There are two general conclusions of importance. First, the distance $r(Z\cdots X)$, where Z is the electron donor atom/centre in the complex B···XY, is smaller than the sum of the van der Waals radii σ_Z and σ_X of these atoms. This result has been shown [179] to be consistent with the conclusion that the van der Waals radius of the atom X in the dihalogen molecule X is shorter along the XY internuclear axis than it is perpendicular to it, i.e. there is a polar flattening of the atom X in the molecule XY of the type suggested by Stone et al. [180]. This result has been shown to hold for the cases XY = Cl_2 [174], BrCl [175], ClF [176] and ICl [178], but not for F_2, in which the F atom in the molecule appears (admittedly on the basis of only a few examples) to be more nearly spherical [177].

The second conclusion concerns the difference $\Delta r = r_{B\cdots HX}(Z\cdots X) - r_{B\cdots XY}(Z\cdots X)$ between the Z to X distances in the two series B···HX and B···XY. Δr is positive and nearly constant for a given B and X, when XY is Cl_2, Br_2, BrCl or ClF. Since the order of the internuclear distances is $r(XY) > r(HX)$ for any given atom X, this result means the outer atom Y of the dihalogen molecule XY is always more distant from a given point in B for the complex B···XY than is the atom X from the same reference point in B for the complex B···HX. This second general result is relevant to the discussion of linear versus non-linear hydrogen and halogen bonds in Sect. 6.

4
Intermolecular Binding Strength in Halogen-Bonded Complexes: Systematic Behaviour of k_σ

The quadratic intermolecular stretching force constant k_σ provides a measure of the force required for a unit infinitesimal increase in the separation of the subunits B and XY along the intermolecular bond in complexes B···XY and hence is one criterion of binding strength. Values can be determined from centrifugal distortion constants D_J or Δ_J using the expressions set out by Millen [26], who assumed a model involving rigid, unperturbed subunits. In practice, this model implies that the complexes are weakly interacting, that the intermolecular stretching mode has a much smaller force constant than any other stretching mode, and that the geometrical perturbations of the subunits are negligible. Strictly, the expressions apply only to complexes in which the halogen bond coincides with the principal inertia axis a (e.g. to complexes of C_{2v} and C_{3v} symmetry here). The heavy atoms S···X – Y in H_2S···XY com-

plexes lie so nearly along the *a* axis that the expressions can also be applied in such cases with insignificant error. We seek the answers to two questions: (1) Are the complexes B···XY weakly bound according to the k_σ criterion? (2) Are there any systematic relationships between the k_σ values as B and XY are varied?

Table 2 displays the values of k_σ for some B···XY complexes of either axial symmetry or C_{2v} symmetry and also those for H_2S···XY, where B is one of several Lewis bases and X is F_2, ClF, Cl_2, BrCl, Br_2 or ICl. These values are taken from papers referred to earlier. It is evident from Table 2 that, for a given XY, the order of k_σ is $N_2 < OC < HCCH \sim H_2CCH_2 \sim HCN < H_2O \sim PH_3 < H_2S < NH_3$. Moreover, for a given B, the order of k_σ is $F_2 < Cl_2 < Br_2 < BrCl < ClF < ICl$, although the number of data for complexes B···F_2 is small.

It has been shown [181] that the hydrogen bond interaction in complexes B···HX are of the weak, predominantly electrostatic type and that the k_σ values in a large number of complexes can be reproduced by means of the empirical equation:

$$k_\sigma = cNE\,, \tag{4}$$

where *N* and *E* are numbers representing the gas-phase nucleophilicities and electrophilicities of the individual molecules B and HX, respectively, and *c* is a constant arbitrarily assigned the value $0.25\,\mathrm{N\,m^{-1}}$. Values of *N* and *E* for a range of B and HX [181] are given in Table 3. The observed and predicted values of k_σ for various B···HX are included in [181] and illustrate that Eq. 4 gives good agreement with the experimental values. Examination of the data in [181] and Table 2 shows that the k_σ for two types of complex B···HX and B···XY are similar in magnitude and that most complexes B···XY are weakly

Table 2 Values of k_σ (in $\mathrm{N\,m^{-1}}$) for series of complexes B···XY and those (in parentheses) calculated using the values of N_B and E_{XY} from Table 4 and Eq. 4

B	XY					
	F_2	Cl_2	Br_2	BrCl	ClF	ICl
N_2	···	···(2.1)	···(3.2)	4.4(3.9)	5.0(4.3)	5.4(5.3)
CO	···	3.7(3.3)	5.1(4.8)	6.3(5.9)	7.0(6.6)	8.0(8.0)
C_2H_2	···	5.6(4.9)	7.8(7.2)	9.4(8.9)	10.0(9.8)	12.1(12.0)
C_2H_4	···	5.9(5.7)	8.8(8.4)	10.5(10.4)	11.0(11.5)	14.0(14.0)
HCN	2.6	6.6(5.9)	···(8.7)	11.1(10.7)	12.3(11.9)	14.5(14.5)
H_2O	3.7	8.0(6.4)	9.8(9.4)	12.1(12.2)	14.2(13.5)	15.7(16.5)
H_2S	2.4	6.3(6.8)	9.8(9.9)	12.2(12.2)	13.3(13.5)	16.6(16.5)
PH_3	···	5.6(6.4)	9.8(9.5)	11.6(11.7)	···(25.0)	20.7(15.8)
NH_3	4.7	12.7(12.5)	18.5(18.3)	26.7(22.6)	34.3(25.0)	30.4(30.5)

Table 3 Nucleophilicities N_B of Lewis bases B and electrophilicities E_{HX} of hydrogen halides HX

B	N_2	CO	C_2H_2	C_2H_4	H_2S	PH_3	HCN	H_2O	NH_3
N_B	2.1	3.4	5.1	4.7	4.8	5.4	7.3	10.0	12.2
HX	HF	HCl	HBr						
E_{HX}	10.0	5.0	4.2						

bound according to this criterion. It is of interest to examine whether the k_σ of the B···XY series can be reproduced by assigning electrophilicities to the various dihalogen molecules. The complexes B···F_2 are excluded from this analysis because of insufficient k_σ values. We assume that c in Eq. 4 has the same value (0.25 N m^{-1}) for both the B···HX and B···XY series and make the arbitrary choice that $E_{ICl} = 10.0$. We then use k_σ for the B···ICl series [93–102] in Eq. 4 to obtain the N_B values for N_2, CO, C_2H_2, C_2H_4, HCN, H_2O, H_2S and NH_3 shown in Table 4.

Table 4 Nucleophilicities N_B of Lewis bases B and electrophilicities E_{XY} of dihalogens XY

B	N_2	CO	C_2H_2	C_2H_4	HCN	H_2O	PH_3	H_2S	NH_3
N_B	2.1	3.2	4.8	5.6	5.8	6.3	6.3	6.6	12.2
XY		Cl_2	Br_2	BrCl	ClF	ICl			
E_{XY}		4.1	6.0	7.4	8.2	10.0			

We do not use k_σ for H_3P···ICl [102] to obtain N_{PH_3} because the k_σ for this complex is anomalously high [20.7(1) N m^{-1}]. Figure 19 shows the straight line that necessarily results for the B···ICl series when k_σ is plotted against N_B. Also shown in Fig. 19 are the results for the other series B···XY, where XY is Cl_2, ClF, BrCl and Br_2, when the N_B values determined from the series B···ICl are used with the appropriate k_σ values. We note that for each series the points lie on a reasonable straight line, the slope of which is, according to Eq. 4, cE_{XY}. Each line drawn results from a least-squares fit and leads to the values E_{XY} for XY = Cl_2, Br_2, BrCl and ClF included in Table 4. The value of $N_B = 6.3$ used for PH_3 was that obtained by requiring that the k_σ for H_3P···Cl_2, H_3P···Br_2 and H_3P···BrCl fitted best onto the existing straight lines for B···Cl_2, B···Br_2 and B···BrCl, respectively. The anomalous nature of the point for H_3P···ICl (added subsequently) is then obvious. The k_σ values for H_3N···ClF and H_3N···BrCl were not included in the least-squares fit for the series B···ClF and B···BrCl, respectively, because they also appear to be anomalously high. These high values are thought to arise from a non-negligible charge transfer, as represented by a small contribution of the ionic structure $[H_3NX]^+$···Y^- to the valence bond description of these complexes (discussed in Sect. 5.2) [52, 63].

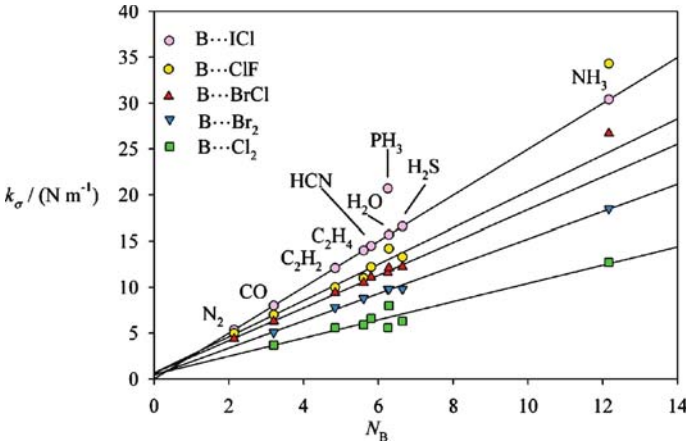

Fig. 19 Variation of the intermolecular stretching force constant k_σ with nucleophilicity N_B for several series of halogen-bonded complexes B···XY, where B is one of a series of Lewis bases and XY is Cl_2, Br_2, BrCl, ClF or ICl. N_B were assigned by use of Eq. 4 with the choice of $E_{ICl} = 10.0$, hence the perfect straight line for the B···ICl series. The lines for the other series are those obtained by least-squares fits to the k_σ values using the N_B determined from the B···ICl series. Points for H_3P···ICl, H_3N···ClF and H_3N···BrCl are anomalous and were excluded from the fits (see text for discussion)

A comparison of the N_B values determined from the B···HX series (Table 3) with those determined here for the B···XY series (Table 4) reveals that the magnitude of N_B obtained in the two different ways is similar for a given B. The notable exception is H_2O, which appears to have a significantly greater nucleophilicity when determined using the B···HX series than it has with respect to halogen or interhalogen diatomic molecules. The order of the electrophilicities of the dihalogen molecules determined as outlined above is $E_{Cl_2} < E_{Br_2} < E_{BrCl} < E_{ClF} < E_{ICl}$ and is reasonable in view of the fact that ICl, ClF and BrCl have small electric dipole moments of $4.14(6) \times 10^{-30}$ C m [182], 2.962×10^{-30} C m [183] and $1.731(12) \times 10^{-30}$ C m [184], respectively, while Cl_2 and Br_2 are non-polar but have electric quadrupole moments of $10.79(54) \times 10^{-40}$ C m^2 [185] and 17.52×10^{-40} C m^2 [186], respectively.

5
Extent of Electron Transfer in Halogen-Bonded Complexes B···XY

5.1
Electron Transfer in Weak (Outer) Complexes B···XY

In Sect. 2, it was indicated that changes $\Delta\chi_{\alpha\beta}(X)$ and $\Delta\chi_{\alpha\beta}(Y)$ in halogen nuclear quadrupole coupling constants $\chi_{\alpha\beta}(X)$ and $\chi_{\alpha\beta}(Y)$ of a dihalogen

molecule XY that accompany formation of B···XY lead directly to the changes in the efgs at X and Y. In turn, the changes in the efgs at X and Y can be interpreted in terms of a simple model to give quantitative information about the electric charge redistribution within XY that attends formation of B···XY. We briefly discuss how the extents of intermolecular electron transfer $\delta_i(B \rightarrow X)$ and intramolecular molecular electron transfer $\delta_p(X \rightarrow Y)$ can be extracted from the observed nuclear quadrupole coupling constants of X and Y. Townes and Dailey [187] developed a simple model for estimating efgs at nuclei, and hence nuclear quadrupole coupling constants, in terms of the contributions from the electrons in a molecule such as XY. First, they assume that filled inner shells of electrons remained spherically symmetric when a molecule XY is formed from the atoms X and Y and, second, they make a similar assumption for valence-shell s electrons. Accordingly, filled inner shells and valence s electrons contribute nothing to efgs, which therefore arise only from p, d, ... valence shell electrons. Moreover, because the contribution of a particular electron to the efg at a given nucleus varies as $\langle r^{-3} \rangle$, where r is the instantaneous distance between the nucleus and the electron, only electrons centred on the nucleus in question contribute significantly to the efg at that nucleus.

We assume that, on formation of B···XY, a fraction δ_i (i = intermolecular) of an electronic charge is transferred from the electron donor atom of Z of the Lewis base B to the np_z orbital of X and that similarly a fraction δ_p (p = polarisation) of an electronic charge is transferred from np_z of X to $n'p_z$ of Y, where z is the XY internuclear axis and n and n' are the valence-shell principal quantum numbers of X and Y. Within the approximations of the Townes–Dailey model [187], the nuclear quadrupole coupling constants at X and Y in the hypothetical equilibrium state of B···XY can be shown [178] to be given by:

$$\chi^{e}_{zz}(X) = \chi_0(X) - (\delta_i - \delta_p)\chi_A(X) \tag{5}$$

and

$$\chi^{e}_{zz}(Y) = \chi_0(Y) - \delta_p \chi_A(Y)\,. \tag{6}$$

In Eqs. 5 and 6, $\chi_0(X)$ and $\chi_A(X)$ are the coupling constants associated with the free molecule XY and the free atom X, respectively, and similar definitions hold for $\chi_0(Y)$ and $\chi_A(Y)$. The free molecule values are known for Cl_2 [188], BrCl [189], Br_2 [190] and ICl [93], as are the free atom coupling constants for Cl, Br and I [191]. The equilibrium coupling constants $\chi^{e}_{zz}(X)$ and $\chi^{e}_{zz}(Y)$ are not observables. The observed (zero-point) coupling constant $\chi_{aa}(X)$ for B···XY is the projection of the equilibrium value $\chi^{e}_{zz}(X)$ onto the principal inertia axis a resulting from the angular oscillation β of the XY subunit about its own centre of mass when within the complex B···XY. If the motion of the B subunit does not change the efgs at X and Y (which is likely to be a good approximation here) $\chi_{aa}(X)$ and $\chi_{aa}(Y)$ are given by the

expressions:

$$\chi_{aa}(\mathrm{X}) = \chi^{\mathrm{e}}_{zz}(\mathrm{X})\,\langle P_2(\cos\beta)\rangle \ , \tag{7}$$

$$\chi_{aa}(\mathrm{Y}) = \chi^{\mathrm{e}}_{zz}(\mathrm{Y})\,\langle P_2(\cos\beta)\rangle \ , \tag{8}$$

in which β is the instantaneous angle between a axis and the XY internuclear axis z and $\langle P_2(\cos\beta)\rangle$ is the second Legendre coefficient. Substitution of Eqs. 7 and 8 into Eqs. 5 and 6 leads to the following expressions for δ_{i} and δ_{p}, the fractions of an electronic charge transferred from B to X and from X to Y, respectively, when B···XY is formed:

$$\delta_{\mathrm{p}} = \frac{\chi_0(\mathrm{Y})}{\chi_{\mathrm{A}}(\mathrm{Y})} - \frac{\chi_{aa}(\mathrm{Y})}{\chi_{\mathrm{A}}(\mathrm{Y})}\,\langle P_2(\cos\beta)\rangle^{-1} \tag{9}$$

$$\delta_{\mathrm{i}} = \frac{\chi_0(\mathrm{X})}{\chi_{\mathrm{A}}(\mathrm{X})} + \frac{\chi_0(\mathrm{Y})}{\chi_{\mathrm{A}}(\mathrm{Y})} - \left\{ \frac{\chi_{aa}(\mathrm{X})}{\chi_{\mathrm{A}}(\mathrm{X})} + \frac{\chi_{aa}(\mathrm{Y})}{\chi_{\mathrm{A}}(\mathrm{Y})} \right\} \langle P_2(\cos\beta)\rangle^{-1} \ . \tag{10}$$

Hence, the inter- and intramolecular electron transfer $\delta_{\mathrm{i}}e$ and $\delta_{\mathrm{p}}e$ can be determined once the value of $P_2(\cos\beta)$ is available. It has been possible to make good estimates of the last quantity for members of each of the series B···Cl_2, B···BrCl, B···Br_2 and B···ICl as follows. By making the reasonable assumption that $\delta_{\mathrm{i}} = 0$ in the weak complexes Ar···BrCl [57] and Ar···ICl [93], the values $\beta_{\mathrm{av}} = \cos^{-1}\left\langle\cos^2\beta\right\rangle^{1/2} = 6.4°$ and 5.4°, respectively, and $\delta_{\mathrm{p}} = 0.0035(6)$ and 0.0054(1), respectively, are determined. The very small values of δ_{p} justify, a posteriori, the assumption $\delta_{\mathrm{i}} = 0$ initially. All other complexes B···BrCl and B···ICl considered are much more strongly bound than Ar···BrCl and Ar···ICl, respectively, and so smaller values of β_{av} (in the range of 5.0(5)° and 4.0(5)°, respectively) were assumed. Moreover, $\langle P_2(\cos\beta)\rangle$ is close to unity even for the Ar complexes and changes so slowly as β_{av} deceases that any errors incurred by such assumptions are negligible. A similar treatment was employed for B···Br_2 and B···Cl_2 complexes using OC···Br_2 [87] and OC···Cl_2 [39] as the complexes appropriate to the weak limit having $\delta_{\mathrm{i}} = 0$, in the absence of experimental knowledge of linear complexes Ar···Br_2 and Ar···Cl_2. Hence, values of δ_{i} and δ_{p} have been determined for the four series B···XY, where B is N_2, CO, C_2H_2, C_2H_4, PH_3, H_2S, HCN, H_2O and NH_3 and XY is Cl_2, Br_2, BrCl and ICl. Some systematic trends are evident in δ_{i} and δ_{p}.

Figure 20 displays plots of δ_{i} against the first ionisation potential I_{B} of the Lewis base B for each of the three series B···Cl_2, B···BrCl [55] and B···ICl [178]. Each set of points can be fitted reasonably well by a function $\delta_{\mathrm{i}} = A\exp(-\,a\,I_{\mathrm{B}})$. This function is shown by a continuous line in each case. The points for the series B···Br_2 lie very close to those for the B···BrCl series and are omitted for clarity.

Figure 20 demonstrates that there is a family relationship among the curves and that the smaller the energy required to remove the most loosely

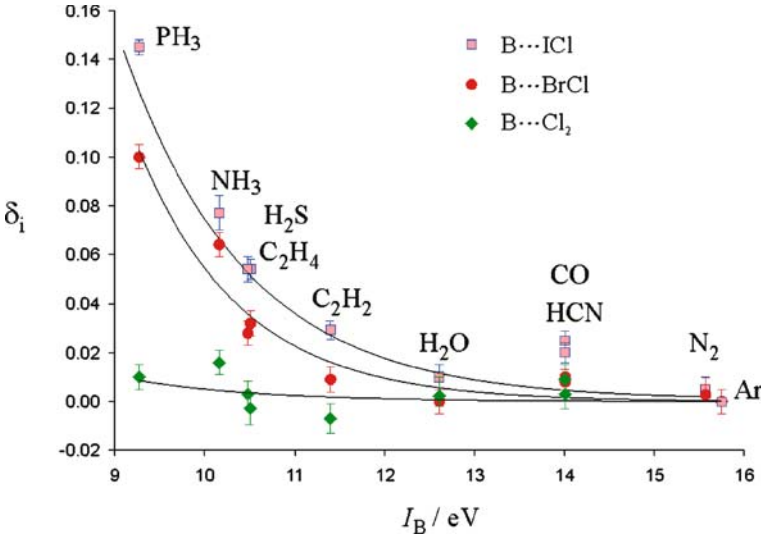

Fig. 20 Variation of the fraction δ_i of an electronic charge transferred from B to XY on formation of B···XY with the ionisation energy I_B of B for the series XY = Cl_2, BrCl and ICl. See text for the method of determination of δ_i from observed XY nuclear quadrupole coupling constants. The *solid curves* are the functions $\delta_i = A \exp(-aI_B)$ that best fit the points for each series B···XY. Data for B···Br_2 are nearly coincident with those of B···BrCl and have been excluded for the sake of clarity

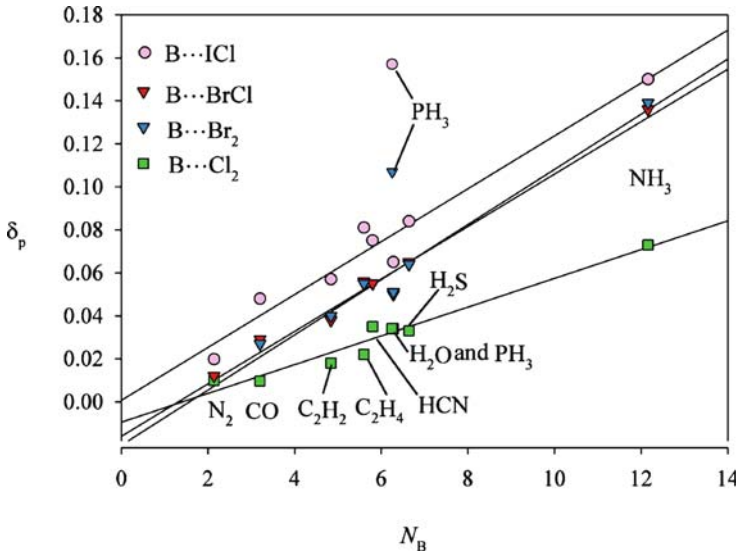

Fig. 21 Variation of the fraction δ_p of an electronic charge transferred from X to Y on formation of B···XY with k_σ for the series XY = Cl_2, Br_2, BrCl and ICl. See text for the method of determination of δ_p from observed XY nuclear quadrupole coupling constants. The *solid line* represents the least-squares fit of the points for each B···XY series

bound electron (n-type or π-type) from B, the greater is the extent of electron transfer from B to XY on formation of B···XY. It is also clear that for all members of the B···Cl_2 series the intermolecular charge transfer is negligible, except possibly for B = NH_3. For a given B, the order of the extent $\delta_i e$ of electron transfer is Cl_2 < Br_2∼BrCl < ICl. Values of δ_i have also been calculated using ab initio methods by several authors [132, 192–195]. In summary, these ab initio calculations lead to values of δ_i of the same order of magnitude as those obtained experimentally and show similar trends as B and XY are varied. The conclusion from both experiments and ab initio calculations is that the extent of electron transfer is generally < 0.06 *e*, except when B = NH_3 and PH_3 and XY = BrCl and ICl.

The values of δ_p also behave systematically, as shown in Fig. 21, in which δ_p is plotted against k_σ for the various series B···XY. It is evident that, for a given XY, δ_p is an approximately linear function of k_σ and hence of the strength of the interaction. Moreover, for a given B the order of δ_p is ICl > BrCl ∼ Br_2 > Cl_2, which is the order of the polarisabilities of the leading atoms X in B···XY and therefore seems reasonable from the definition (see earlier) of δ_p.

5.2
Do Mulliken Inner Halogen-Bonded Complexes Exist in the Gas Phase?

A detailed analysis of the halogen and nitrogen nuclear quadrupole coupling constants for the series of hydrogen-bonded complexes$(CH_3)_{3-n}H_nN\cdots HX$, where $n = 0$ and 3 and X = F, Cl, Br and I, has allowed conclusions about how the extent of proton transfer changes with both n and X. The work has been reviewed in detail elsewhere [196] and only a summary is given here. It was concluded that progressive methylation of ammonia, which leads to a monotonic increase in the gas-phase proton affinity of the base, coupled with a decrease in the energy change accompanying the gas-phase process $HX = H^+ + X^-$ along the series X = F, Cl, Br and I, allows the Mulliken inner complex $[(CH_3)_{3-n}H_nNH]^+\cdots X^-$ to become more stable than the Mulliken outer complex $(CH_3)_{3-n}H_nN\cdots HX$ when X = Br and I and $n = 0$. In fact, the extent of proton transfer was crudely estimated to be ∼0%, ∼60%, ∼80% and ∼100% for the series $(CH_3)_3N\cdots HX$, when X is F, Cl, Br and I, respectively, a result which indicates that the proton is gradually transferred as HX becomes progressively easier to dissociate in the case when the proton affinity of the base is greatest. Is there any evidence for Mulliken inner complexes $[BX]^+\cdots Y^-$?

Evidence for a significant contribution from the ionic form $[BX]^+\cdots Y^-$ in a gas-phase complex B···XY was first deduced from the spectroscopic constants of $H_3N\cdots ClF$, as obtained by analysis of its rotational spectrum [63]. In particular, the value $k_\sigma = 34.3\ N\ m^{-1}$ of the intermolecular stretching force constant (obtained from the centrifugal distortion constant D_J in the man-

ner outlined in Sect. 2 is large compared with that (ca. 25 N m^{-1}) expected from the plot of k_σ versus N_B shown in Fig. 19. Similarly, the Cl-nuclear quadrupole coupling constant is smaller in magnitude than those of more weakly bound B···ClF complexes. A detailed analysis suggested [63, 68] a contribution of $H_3NCl^+\cdots F^-$ of roughly 20% to the valence bond description of $H_3N\cdots ClF$.

In view of the fact that complete methylation of $H_3N\cdots HX$ to give $(CH_3)_3N\cdots HX$ leads to an increased extent of proton transfer from HX to the base when X is Cl and essentially complete transfer when X is I, it seemed reasonable to seek a more significant contribution from the ionic valence bond structure $[(CH_3)_3NCl]^+\cdots F^-$ in $(CH_3)_3N\cdots ClF$ by examining properties similarly derived from its rotational spectrum [68].

It was found that $(CH_3)_3N\cdots ClF$ has a centrifugal distortion constant D_J consistent with the large value $k_\sigma \sim 70$ N m^{-1} for the intermolecular stretching force constant. The distance $r(N\cdots Cl) = 2.090$ Å, as obtained by isotopic substitution at N and Cl, is very short compared with that predicted for an intermolecular N···Cl bond in an analogous complex in which little ionic character is expected, for example HCN···ClF [64], which is weakly bound ($k_\sigma = 12.3$ N m^{-1}) and has $r(N\cdots Cl) = 2.639(3)$ Å. The Cl nuclear quadrupole coupling constant of $(CH_3)_3N\cdots ClF$ is significantly smaller in magnitude than expected of a weakly bound complex. A detailed analysis of the observed coupling constant leads to an estimated contribution of ca. 60% for the ionic valence bond structure $[(CH_3)_3NCl]^+\cdots F^-$. In addition, the ^{14}N nuclear quadrupole coupling constant of $(CH_3)_3N\cdots ClF$ is consistent with a substantial (roughly 70%) contribution of the ion-pair form. It should be emphasised that the models used to interpret the Cl and N nuclear quadrupole coupling constants were crude and that the percentage ionic characters deduced thereby are only semi-quantitative. Nevertheless, there is evidence of a substantial (∼50%) contribution from the ionic structure $[(CH_3)_3NCl]^+\cdots F^-$ in a valence-bond description. Hence, $(CH_3)_3N\cdots ClF$ appears to be intermediate between a Mulliken outer and inner complex. These experimental conclusions are consistent with the results of ab initio calculations [197, 198].

A detailed examination of the rotational spectrum $(CH_3)_3N\cdots F_2$ led [37] to molecular properties that suggest that this complex too has significant ion-pair character. Thus, the behaviour of the spectral intensity as a function of microwave radiation power led to an estimate of ∼10 D for the electric dipole moment, a value which is an order of magnitude large than that (∼1 D) expected on the basis of the vector sum of the component dipole moments (i.e. with no charge transfer). The centrifugal distortion constant D_J is consistent with a large intermolecular stretching force constant k_σ. The value of the ^{14}N-nuclear quadrupole coupling constant implies a substantial contribution from $[(CH_3)_3NF]^+\cdots F^-$, as do all the other properties mentioned. If the complex is assumed to be entirely $[(CH_3)_3NF]^+\cdots F^-$ and the geom-

etry of trimethylamine is assumed to be unchanged when F_2 approaches it along the C_3 axis to form $[(CH_3)_3NF]^+\cdots F^-$, the observed ground-state moments of inertia of the three isotopomers $(CH_3)_3{}^{14}N\cdots F_2$, $(CH_3)_3{}^{15}N\cdots F_2$ and $(CD_3)_3{}^{14}N\cdots F_2$ can be fitted to give the distances $r(N-F) = 1.29(4)$ Å and $r(F-F) = 2.32(4)$ Å, a result consistent with significant covalent character of the N – F bond, with a substantially lengthened F – F bond, and therefore with an ion-pair type of structure. Subsequent ab initio calculations [197–199] showed that this approach overestimates the ionic character, largely because the trimethylamine geometry is significantly perturbed on formation of the complex. If this perturbed geometry of trimethylamine is used in place of the unperturbed geometry and the observed experimental moments of inertia are refitted, the revised bond lengths involving fluorine are $r(N-F) = \sim 1.7$ Å and $r(F-F) = \sim 1.9$ Å, which are in good agreement with the ab initio values [199]. Evidently the $(CH_3)_3N\cdots F_2$ complex has a significant ion-pair character. We conclude therefore that even in the gas phase there are complexes, such as $(CH_3)_3N\cdots ClF$ and $(CH_3)_3N\cdots F_2$, for which the description "inner complex" is partially appropriate.

6
Conclusions: A Model for the Halogen Bond in B···XY

We have established in Sect. 3 a strong case to support the conclusion that a complex B···XY involving a given Lewis base B and a dihalogen molecule XY has an angular geometry that is isomorphous with that of the corresponding member of the series of hydrogen-bonded complexes B···HX. This was achieved mainly by a comparison of pairs of complexes B···HCl and B···ClF for a given B, coupled with the systematic variation of the Lewis base, although there is also similar, but less complete, evidence from comparisons of other series B···HX and B···XY, where X is Cl, Br or I and Y is Cl or Br. The observed parallelism among angular geometries of B···HX and B···XY suggests that the empirical rules [103, 104] for predicting angular geometries of hydrogen-bonded complexes B···HX can be extended to halogen-bonded complexes B···XY. The polarity of the heteronuclear dihalogen molecules ClF, BrCl and ICl is such that the more electropositive atom of each pair, i.e. Cl, Br and I, respectively, carries a small net positive charge $^{\delta+}$ while the other atom carries a corresponding net negative charge $^{\delta-}$. Although the homonuclear dihalogen molecules F_2, Cl_2 and Br_2 have no electric dipole moment, each has a non-zero electric quadrupole moment that can be represented by the following electric charge distribution: $^{\delta+}X\underline{\overline{^{\delta-}}}X^{\delta+}$. Thus we can envisage the partial positive charge $^{\delta+}$ associated with the atom X in XY or X_2 as interacting with a n- or a π-electron pair on the Lewis base B when we restate the rules for halogen-bonded complexes B···XY as follows:

The equilibrium angular geometry of a halogen-bonded complex B···XY can be predicted by assuming that the internuclear axis of a XY or X_2 molecule lies:

1. Along the axis of a non-bonding (n) electron pair carried by the acceptor atom Z of B, with order of atoms $Z\cdots{}^{\delta+}X - Y^{\delta-}$, or
2. Along the local symmetry axis of a π or pseudo-π orbital if B carries only π-pairs, or
3. Along the axis of a n-pair when B carries both n- and π-pairs (i.e. rule 1 takes precedence)

The main difference between hydrogen bond and the halogen bond lies in the propensity of the hydrogen bond to be non-linear [28, 29], when symmetry of the complex is appropriate (molecular point group C_S or C_1). In so far as complexes B···ClF are concerned, the nuclei Z···Cl – F, where Z is the acceptor atom/centre in B, appear to be nearly collinear in all cases, while the nuclei Z···H – Cl in complexes B···HCl of appropriate symmetry often show significant deviations from collinearity. This propensity for the hydrogen-bonded species B···HCl to exhibit non-linear hydrogen bonds can be understood as follows.

We imagine that $^{\delta+}H–Cl^{\delta-}$ approaches B, $^{\delta+}H$ first, along the axis of, e.g., an n-pair, as required by the rules. Then a secondary attraction, between the nucleophilic end $Cl^{\delta-}$ of HCl and the most electrophilic region E of B, causes $Cl^{\delta-}$ to move towards E but with $^{\delta+}H$ fixed, so that the motion is pivoted at $^{\delta+}H$. The angle Z···H – Cl (defined as ϕ in most of the figures) therefore remains constant in first approximation, which explains why the values of ϕ in complexes B···HCl are those predicted by the rules even though the hydrogen bond is non-linear. In the new equilibrium position the force of attraction between E and $Cl^{\delta-}$ is balanced by the force tending to restore the hydrogen bond to linearity. There are three factors that conspire to keep the Z···Cl – F nuclei in B···ClF more nearly collinear than the nuclei Z···H – Cl in the corresponding complex B···HCl:

1. For a given B, the Z···Cl bond in B···ClF is stronger than the Z···H bond in B···HCl (as measured by k_σ) and is presumably more difficult to bend
2. $Cl^{\delta-}$ in HCl is probably a better nucleophile than $F^{\delta-}$ of ClF
3. $F^{\delta-}$ is further away from the electrophilic region E of B than is $Cl^{\delta-}$ (see Sect. 3.4)

It is of interest to note that systematic studies [200–204] of complexes B···HCCH involving weak primary hydrogen bonds Z···HCCH have revealed large non-linearities, but with an angle ϕ that remains reasonably close to those predicted by the rules. Figure 22 illustrates this result through the experimentally determined geometries for the cases when B is 2,5-dihydrofuran [200], oxirane [201], formaldehyde [202], thiirane [203], and vinyl fluoride [204]. On the other hand, as noted in Sect. 3.1.3, both

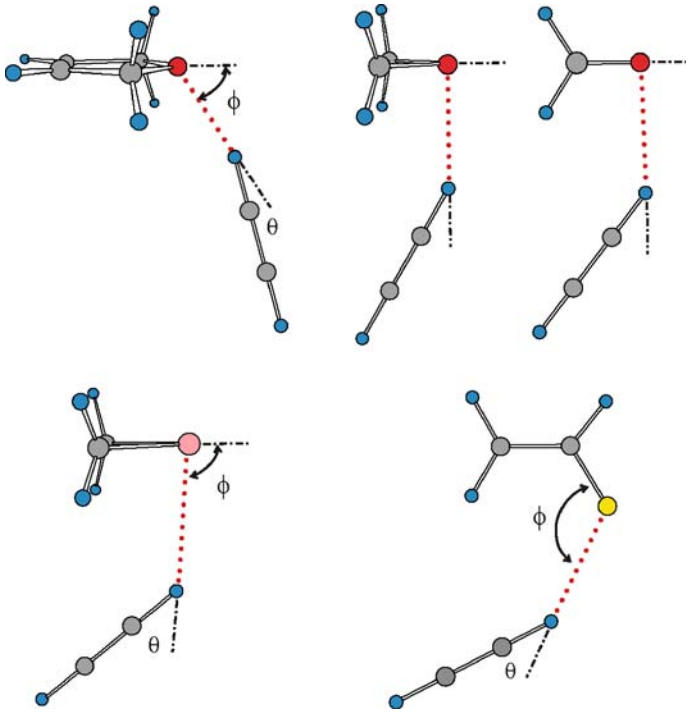

Fig. 22 Experimentally determined geometries, drawn to scale, for a series of weak, hydrogen-bonded complexes B···HCCH, where B is 2,5-dihydrofuran, oxirane, formaldehyde, thiirane or vinyl fluoride. The values of [ϕ and θ] are [57.8(18)° and 16.2(32)°], [90.4(12)° and 29.8(4)°], [92.0(15)° and 39.5(10)°], [96.0(5)° and 42.9(23)°] and [122.6(4)° and 36.5(2)°], respectively. The non-linearities of the hydrogen bonds are large because the primary Z···H hydrogen bonds are weak. The exception is 2,5-dihydrofuran···HCCH, in which the distance between the centre of the ethyne π bond and the most electrophilic region of B is larger because the angle ϕ is smaller than for other B, thus making the secondary interaction correspondingly weaker. See Fig. 1 for key to the colour coding of atoms

SO_2···ClF [70] and SO_2···HCl [28, 126] have negligible non-linearity of the halogen and hydrogen bonds, respectively, even though weakly bound. Examination of Fig. 10 reveals that the $F^{\delta-}$ and $Cl^{\delta-}$ are far away from the centre $S^{\delta+}$ in each case and that, therefore, the linear arrangements are to be expected.

The rules for predicting angular geometries of halogen-bonded complexes B···XY have recently received support from a wide ranging analysis of X-ray diffraction studies in the solid state by Laurence and co-workers [205]. This study not only confirms the validity of the rules in connection with complexes B···XY, where XY is Cl_2, Br_2, I_2, ICl and IBr, with many Lewis bases B but also reinforces the conclusion that halogen bonds Z···X – Y show a smaller propensity to be non-linear that do hydrogen bonds Z···H — X.

There are other parallels between the series of complexes B···XY and B···HX. We established in Sect. 4 that B···XY and B···HX have, in general, similar binding strengths, as measured by the intermolecular stretching force constant k_σ, and both are, for the most part, weakly bound. We have also shown in Sect. 5 that the electric charge redistribution that occurs when B···XY is formed from its components B and XY is generally small (exceptions among both halogen- and hydrogen-bonded complexes were discussed).

The striking parallel behaviour among the various properties of B···XY and B···HX suggests that the origin of the halogen-bond interaction might be similar to that of the hydrogen bond interaction. An electrostatic model has had much success in predicting angular geometries, both qualitatively [103, 104] and quantitatively [206]. In first approximation, an electrostatic model is one which takes into account only the interaction of the unperturbed electric charge distributions of the two component molecules as they come together to form the complex in its equilibrium conformation, with contributions from interactions of any induced moments assumed minor. The empirical rules set out in Sect. 3 and this section for hydrogen-bonded and halogen-bonded complexes, respectively, are inherently electrostatic in origin. The reason why the electrostatic component of the energy is definitive of the angular geometry has been investigated in detail through ab initio calculations [207] for $H_2O\cdots HF$. The systematic behaviour of the intermolecular force constants k_σ of hydrogen-bonded complexes has been discussed in terms of a predominantly electrostatic interpretation [181].

References

1. Guthrie F (1863) J Chem Soc 16:239
2. Benesi HA, Hildebrand JH (1949) J Am Chem Soc 71:2703
3. Mulliken RS, Person WB (1969) Molecular complexes: A lecture and reprint volume. Wiley-Interscience, New York
4. Hassel O, Rømming C (1962) Quart Rev Chem Soc 16:1
5. Hassel O (1970) Science 170:497
6. Frei H, Pimentel GC (1985) Annu Rev Phys Chem 36:491
7. Bai H, Ault BS (1990) J Phys Chem 94:199
8. Bai H, Ault BS (1990) J Mol Struct 238:223
9. Machara NP, Ault BS (1988) J Mol Struct 172:126
10. Machara NP, Ault BS (1988) Inorg Chem 27:2383
11. Andrews L, Hunt RD (1988) J Chem Phys 89:3502
12. Andrews L, Lascola R (1987) J Am Chem Soc 109:6243
13. Andrews L, McInnis TC, Hannachi Y (1992) J Phys Chem 96:4248
14. McInnis TC, Andrews L (1992) J Phys Chem 96:2051
15. Legon AC, Rego CA (1990) J Chem Soc Faraday Trans 86:1915
16. Balle TJ, Flygare WH (1981) Ann Rev Sci Instrum 52:33
17. Legon AC (1992) In: Scoles G (ed) Atomic and molecular beam methods, vol 2. Oxford University Press, New York, p 289

18. Arunan E et al. (2007) Chemistry International, March–April 2007, available at http://www.iupac.org/publications/ci/2007/2902/pp1_2004-026-2-100.html
19. Legon AC (1999) Angew Chem Int Ed 38:2686
20. Legon AC (1998) Chem Eur J 4:1890
21. Metrangolo P, Neukirch H, Pilati T, Resnati G (2005) Acc Chem Res 38:386
22. Bloemink HI, Dolling SJ, Legon AC (1995) J Chem Soc Faraday Trans 91:2059
23. Legon AC, Millen DJ (1986) Chem Rev 86:635
24. Leopold KR, Fraser GT, Novick SE, Klemperer W (1994) Chem Rev 94:1807
25. Legon AC (1992) J Mol Struct 266:21
26. Millen DJ (1985) Can J Chem 63:1477
27. Townes CH, Schawlow AL (1955) Microwave spectroscopy. McGraw-Hill, New York, p 149
28. Legon AC (1994) Faraday Discuss Chem Soc 97:19
29. Legon AC, Thorn JC (1994) Chem Phys Lett 227:472
30. Bloemink HI, Hinds K, Holloway JH, Legon AC (1995) Chem Phys Lett 245:598
31. Cooke SA, Cotti G, Evans CM, Holloway JH, Legon AC (1996) Chem Phys Lett 260:388
32. Cooke SA, Cotti G, Evans CM, Holloway JH, Legon AC (1996) Chem Phys Lett 262:308
33. Cooke SA, Cotti G, Holloway JH, Legon AC (1997) Angew Chem Int Ed 36:129
34. Cooke SA, Cotti G, Evans CM, Holloway JH, Kisiel Z, Legon AC, Thumwood JMA (2001) Chem Eur J 7:2295
35. Cotti G, Evans CM, Holloway JH, Legon AC (1997) Chem Phys Lett 264:513
36. Evans CM, Holloway JH, Legon AC (1997) Chem Phys Lett 267:281
37. Bloemink HI, Cooke SA, Holloway JH, Legon AC (1997) Angew Chem Int Ed 36:1340
38. Baiocchi FA, Dixon TA, Klemperer W (1982) J Chem Phys 77:1632
39. Jäger W, Xu Y, Gerry MCL (1993) J Chem Phys 97:3685
40. Legon AC, Warner HE (1993) J Chem Phys 98:3827
41. Legon AC, Thorn JC (1993) J Chem Soc Faraday Trans 89:4157
42. Legon AC, Lister DG, Thorn JC (1994) J Chem Soc Chem Commun, p 757
43. Bloemink HI, Hinds K, Legon AC, Thorn JC (1994) J Chem Soc Chem Commun, p 1321
44. Bloemink HI, Hinds K, Legon AC, Thorn JC (1994) Chem Phys Lett 223:162
45. Legon AC, Lister DG, Thorn JC (1994) J Chem Soc Faraday Trans 90:3205
46. Bloemink HI, Hinds K, Legon AC, Thorn JC (1995) Chem Eur J 1:17
47. Bloemink HI, Cooke SA, Hinds K, Legon AC, Thorn JC (1995) J Chem Soc Faraday Trans 91:1891
48. Davey JB, Legon AC, Thumwood JMA (2001) J Chem Phys 114:6190
49. Blanco S, Legon AC, Thorn JC (1994) J Chem Soc Faraday Trans 90:1365
50. Bloemink HI, Hinds K, Legon AC, Thorn JC (1994) J Chem Soc Chem Commun, p 1229
51. Bloemink HI, Hinds K, Legon AC, Thorn JC (1994) Angew Chem Int Ed 33:1512
52. Bloemink HI, Legon AC, Thorn JC (1995) J Chem Soc Faraday Trans 91:781
53. Hinds K, Legon AC (1995) Chem Phys Lett 240:467
54. Bloemink HI, Legon AC (1996) Chem Eur J 2:265
55. Legon AC, Thumwood JMA, Waclawik ER (2000) J Chem Phys 113:5278
56. Davey JB, Legon AC (2001) Phys Chem Chem Phys 3:3006
57. Davey JB, Legon AC, Waclawik ER (2001) Chem Phys Lett 346:103
58. Legon AC, Ottaviani P (2002) Phys Chem Chem Phys 4:441
59. Janda KC, Steed JM, Novick SE, Klemperer W (1977) 67:5162

60. Bloemink HI, Hinds K, Holloway JH, Legon AC (1995) Chem Phys Lett 242:113
61. Hinds K, Holloway JH, Legon AC (1995) Chem Phys Lett 242:407
62. Bloemink HI, Hinds K, Legon AC, Holloway JH (1995) J Chem Soc Chem Commun, p 1833
63. Bloemink HI, Evans CM, Holloway JH, Legon AC (1996) Chem Phys Lett 248:260
64. Hinds K, Legon AC, Holloway JH (1996) Mol Phys 88:673
65. Bloemink HI, Holloway JH, Legon AC (1996) Chem Phys Lett 250:567
66. Hinds K, Holloway JH, Legon AC (1996) J Chem Soc Faraday Trans 92:1296
67. Bloemink HI, Evans CM, Holloway JH, Legon AC (1996) Chem Phys Lett 251:275
68. Bloemink HI, Holloway JH, Legon AC (1996) Chem Phys Lett 254:59
69. Evans CM, Holloway JH, Legon AC (1996) Chem Phys Lett 255:119
70. Cotti G, Holloway JH, Legon AC (1996) Chem Phys Lett 255:401
71. Cooke SA, Cotti G, Hinds K, Holloway JH, Legon AC, Lister DG (1996) J Chem Soc Faraday Trans 9:2671
72. Cooke SA, Cotti G, Evans CM, Holloway JH, Legon AC (1996) Chem Commun, p 2327
73. Hinds K, Holloway JH, Legon AC (1996) J Chem Soc Faraday Trans 93:373
74. Cooke SA, Holloway JH, Legon AC (1997) J Mol Struct 406:15
75. Cooke SA, Holloway JH, Legon AC (1997) Chem Phys Lett 266:61
76. Cooke SA, Holloway JH, Legon AC (1997) J Chem Soc Faraday Trans 93:2361
77. Cooke SA, Corlett GK, Evans CM, Holloway JH, Legon AC (1997) Chem Phys Lett 275:269
78. Cooke SA, Holloway JH, Legon AC (1997) J Chem Soc Faraday Trans 93:4253
79. Cooke SA, Corlett GK, Evans CM, Legon AC, Holloway JH (1998) J Chem Phys 108:39
80. Cooke SA, Evans CM, Holloway JH, Legon AC (1998) J Chem Soc Faraday Trans 94:2295
81. Cooke SA, Corlett GK, Holloway JH, Legon AC (1997) J Chem Soc Faraday Trans 94:2675
82. Waclawik ER, Legon AC, Holloway JH (1998) Chem Phys Lett 295:289
83. Cooke SA, Holloway JH, Legon AC (1998) Chem Phys Lett 298:151
84. Page MD, Waclawik ER, Holloway JH, Legon AC (1999) J Mol Struct 509:55
85. Davey JB, Holloway JH, Legon AC, Waclawik ER (1999) Phys Chem Chem Phys 1:2415
86. Bloemink HI, Legon AC (1995) J Chem Phys 103:876
87. Waclawik ER, Thumwood JMA, Lister DG, Fowler PW, Legon AC (1999) Mol Phys 97:159
88. Waclawik ER, Legon AC (2000) Chem Eur J 6:3968
89. Legon AC, Thumwood JMA (2001) Phys Chem Chem Phys 3:1397
90. Legon AC, Thumwood JMA (2001) Phys Chem Chem Phys 3:2758
91. Legon AC, Thumwood JMA, Waclawik ER (2002) Chem Eur J 8:940
92. Davey JB, Legon AC (2001) Chem Phys Lett 350:39
93. Davey JB, Legon AC, Waclawik ER (1999) Chem Phys Lett 306:133
94. Davey JB, Legon AC, Waclawik ER (1999) Phys Chem Chem Phys 1:3097
95. Davey JB, Legon AC (1999) Phys Chem Chem Phys 1:3721
96. Thumwood JMA, Legon AC (1999) Chem Phys Lett 310:88
97. Waclawik ER, Legon AC (1999) Phys Chem Chem Phys 1:4695
98. Legon AC, Waclawik ER (1999) Chem Phys Lett 312:385
99. Herrebout WA, Legon AC, Waclawik ER (1999) Phys Chem Chem Phys 1:4961
100. Davey JB, Legon AC, Waclawik ER (2000) J Mol Struct 500:391
101. Davey JB, Legon AC, Waclawik ER (2000) Phys Chem Chem Phys 2:1659

102. Davey JB, Legon AC, Waclawik ER (2000) Phys Chem Chem Phys 2:2265
103. Legon AC, Millen DJ (1982) Faraday Discuss Chem Soc 73:71
104. Legon AC, Millen DJ (1987) Chem Soc Rev 16:467
105. Howard NW, Legon AC (1988) J Chem Phys 88:4694
106. Howard NW, Legon AC (1987) J Chem Phys 86:6722
107. Legon AC, Stephenson D (1992) J Chem Soc Faraday Trans 88:761
108. Legon AC, Thumwood JMA, Waclawik ER, Willoughby LC (2000) Phys Chem Chem Phys 2:4918
109. Willoughby LC, Legon AC (1983) J Phys Chem 87:2085
110. Howard NW, Legon AC, Luscombe GJ (1991) J Chem Soc Faraday Trans 87:507
111. Bevan JW, Kisiel Z, Legon AC, Millen DJ (1980) Proc Roy Soc Lond A 372:441
112. Kisiel Z, Legon AC, Millen DJ (1982) Proc Roy Soc Lond A 381:419
113. Legon AC, Willoughby LC (1983) Chem Phys Lett 95:449
114. Kisiel Z, Pietrewicz BA, Fowler PW, Legon AC, Steiner E (2000) J Phys Chem 104:6970
115. Legon AC, Suckley AP (1988) Chem Phys Lett 150:153
116. McIntosh A, Walther T, Lucchese RR, Bevan JW, Suenram RD, Legon AC (1999) Chem Phys Lett 314:57
117. Willougby LC, Fillery-Travis AJ, Legon AC (1984) J Chem Phys 81:20
118. Goodwin EJ, Legon AC (1984) J Chem Soc Faraday Trans 2 80:51
119. Jaman AI, Legon AC (1986) J Mol Struct 145:261
120. Legon AC, Rego CA, Wallwork AL (1992) J Chem Phys 97:3050
121. Legon AC (1996) J Chem Soc Faraday Trans 92:2677
122. Antolinez S, Lopez JC, Alonso JL (2001) Chem Phys Lett 334:250
123. Evans CM, Legon AC (1995) Chem Phys 198:119
124. Atkins MJ, Legon AC, Warner HE (1994) Chem Phys Lett 229:267
125. Legon AC, Wallwork AL, Warner HE (1991) J Chem Soc Faraday Trans 87:3327
126. Fillery-Travis AJ, Legon AC (1986) Chem Phys Lett 123:4
127. Fillery-Travis AJ, Legon AC (1986) J Chem Phys 85:3180
128. Aldrich PD, Legon AC, Flygare WH (1981) J Chem Phys 75:2126
129. Shea JA, Flygare WH (1982) J Chem Phys 76:4857
130. Fowler PW, Legon AC, Thumwood JMA, Waclawik ER (2000) Coord Chem Rev 197:231
131. Dubois JE, Garnier F (1967) Spectrochim Acta 23A:2279
132. Lenoir D, Chiappe C (2003) Chem Eur J 9:1037
133. Read WG, Flygare WH (1982) J Chem Phys 76:292
134. Legon AC, Aldrich PD, Flygare WH (1981) J Chem Phys 75:625
135. Cole GC, Davey JB, Legon AC, Lyndon AF (2003) Mol Phys 101:603
136. Coulson CA, Moffitt WE (1949) Philos Mag 40:1
137. Legon AC, Aldrich PD, Flygare WH (1982) J Am Chem Soc 104:1486
138. Buxton LW, Aldrich PD, Shea JA, Legon AC, Flygare WH (1981) J Chem Phys 75:2681
139. Baiocchi FA, Williams JH, Klemperer W (1983) J Phys Chem 87:2079
140. Read WG, Campbell EJ, Henderson G (1983) J Chem Phys 78:3501
141. Cooke SA, Corlett GK, Evans CM, Legon AC (1997) Chem Phys Lett 272:61
142. Legon AC, Willoughby LC (1988) Chem Phys Lett 143:214
143. Kisiel Z, Fowler PW, Legon AC (1994) J Chem Phys 101:4635
144. Kisiel Z, Fowler PW, Legon AC (1995) Chem Phys Lett 232:187
145. Legon AC, Lister DG (1999) Phys Chem Chem Phys 1:4175
146. Legon AC, Soper PD, Flygare WH (1981) J Chem Phys 74:4944
147. Soper PD, Legon AC, Flygare WH (1981) J Chem Phys 74:2138

148. Keenan MR, Minton TK, Legon AC, Balle TJ, Flygare WH (1981) Proc Nat Acad Sci USA 77:5583
149. Wang Z, Lucchese RR, Bevan JW, Suckley AP, Rego CA, Legon AC (1993) J Chem Phys 98:1761
150. Soper PD, Legon AC, Read WG, Flygare WH (1982) J Chem Phys 76:292
151. Altmann RS, Marshall MD, Klemperer W (1983) J Chem Phys 79:57
152. Howard NW, Legon AC (1988) Chem Phys Lett 149:57
153. Howard NW, Legon AC (1989) J Chem Phys 90:672
154. Legon AC, Millen DJ, Rogers SC (1980) Proc Roy Soc Lond A 370:213
155. Legon AC, Millen DJ, Willoughby LC (1985) Proc Roy Soc Lond A 401:327
156. Legon AC, Campbell EJ, Flygare WH (1982) J Chem Phys 76:2267
157. Campbell EJ, Legon AC, Flygare WH (1983) J Chem Phys 78:3494
158. Fowler PW, Legon AC, Peebles SA (1994) Chem Phys Lett 226:501
159. Bevan JW, Legon AC, Millen DJ, Rogers SC (1980) Proc Roy Soc Lond A 370:239
160. Soper PD, Legon AC, Read WG, Flygare WH (1981) J Phys Chem 85:3440
161. Legon AC, Millen DJ, North HM (1987) J Phys Chem 91:5210
162. Kisiel Z, Fowler PW, Legon AC (1990) J Chem Phys 93:3054
163. Cole GC, Legon AC (2004) Chem Phys Lett 400:419
164. Legon AC, Ottaviani P (2002) Phys Chem Chem Phys 4:4103
165. Shea JA, Kukolich SG (1983) J Chem Phys 78:3545
166. Lesarri A, Lopez JC, Alonso JL (1998) J Chem Soc Faraday Trans 94:729
167. Cooke SA, Corlett GK, Legon AC (1998) J Chem Soc Faraday Trans 94:1565
168. Cooke SA, Corlett GK, Legon AC (1998) Chem Phys Lett 291:269
169. Legon AC, Ottaviani P (2004) Phys Chem Chem Phys 6:488
170. Cooke SA, Corlett GK, Legon AC (1998) J Mol Struct 448:107
171. Cooke SA, Corlett GK, Lister DG, Legon AC (1998) J Chem Soc Faraday Trans 94:837
172. Cole GC, Legon AC (2004) J Chem Phys 121:10467
173. Cole GC, Legon AC, Ottaviani P (2002) J Chem Phys 117:2790
174. Legon AC (1995) Chem Phys Lett 237:291
175. Legon AC (1995) J Chem Soc Faraday Trans 91:1881
176. Legon AC (1997) Chem Phys Lett 279:55
177. Legon AC (1998) Chem Commun, p 2737
178. Legon AC (1999) Chem Phys Lett 314:472
179. Peebles SA, Fowler PW, Legon AC (1995) Chem Phys Lett 240:130
180. Price SL, Stone AJ, Lucas J, Rowland RS, Thornley AE (1994) J Am Chem Soc 116:4910
181. Legon AC, Millen DJ (1987) J Am Chem Soc 109:356
182. Herbst E, Steinmetz WE (1972) J Chem Phys 56:5346
183. Fabricant B, Muenter JS (1977) J Chem Phys 66:5274
184. Nair KPR, Hoeft J, Tiemann E (1978) Chem Phys Lett 58:153
185. Buckingham AD, Graham C, Williams JH (1983) Mol Phys 49:703
186. Fowler PW, Legon AC, Peebles SA (1997) Adv Quant Chem 28:247
187. Townes CH, Schawlow AL (1955) Microwave spectroscopy. McGraw-Hill, New York, p 225
188. Xu Y, Jäger W, Ozier I, Gerry MCL (1993) J Chem Phys 98:3726
189. Legon AC, Thorn JC (1993) Chem Phys Lett 215:554
190. Bettin N, Knöckel H, Tiemann E (1981) Chem Phys Lett 80:386
191. Gordy W, Cook RL (1983) Microwave molecular spectra. In: Weissberger A (ed) Techniques of chemistry, vol XVIII, 3rd edn. Wiley, New York, pp 725–802
192. Alkorta I, Rozas I, Elguero E (1998) J Phys Chem A 102:9278

193. Karpfen A (2000) J Phys Chem A 104:6871
194. Zhang Y, Xiao-Zeng Y (2001) J Computat Chem 22:327
195. Zou J-W, Jiang Y-J, Gou M, Hu G-X, Zhang B, Liu H-C, Yu Q-S (2005) Chem Eur J 11:740
196. Legon AC (1993) Chem Soc Rev 22:153
197. Karpfen A (1999) Chem Phys Lett 299:493
198. Domene C, Fowler PW, Legon AC (1999) Chem Phys Lett 309:463
199. Karpfen A (2003) Theor Chem Acc 110:1
200. Cole GC, Hughes RA, Legon AC (2005) J Chem Phys 122:134311
201. Legon AC (1995) Chem Phys Lett 247:24
202. Howard NW, Legon AC (1988) J Chem Phys 88:6793
203. Batten RC, Cole GC, Legon AC (2003) J Chem Phys 119:7903
204. Cole GC, Legon AC (2003) Chem Phys Lett 369:31
205. Ouvrard C, Le Questel J-Y, Berthelot M, Laurence C (2003) Acta Cryst B 59:512
206. Buckingham AD, Fowler PW (1985) Can J Chem 63:2018
207. Hurst GJB, Fowler PW, Stone AJ, Buckingham AD (1986) Int Rev Phys Chem 5:107